Atom diffusion and impurity-induced layer disordering in quantum well III-V semiconductor heterostructures

D. G. Deppe and N. Holonyak, Jr.
Electrical Engineering Research Laboratory, Center for Compound Semiconductor Microelectronics, and Material Research Laboratory, University of Illinois at Urbana-Champaign, Urbana, Illinois 61801

(Received 5 May 1988; accepted for publication 22 August 1988)

The process of impurity-induced layer disordering (IILD) or layer intermixing, in $Al_xGa_{1-x}As$-GaAs quantum well heterostructures (QWHs) and superlattices (SLs), and in related III-V quantum well heterostructures, has developed extensively and is reviewed. A large variety of experimental data on IILD are discussed and provide newer information and further perspective on crystal self-diffusion, impurity diffusion, and also the important defect mechanisms that control diffusion in $Al_xGa_{1-x}As$-GaAs, and in related III-V semiconductors. Based on the behavior of Column III vacancies and Column III interstitials, models for the crystal self-diffusion and impurity diffusion that describe IILD are reviewed and discussed. Because impurity-induced layer disordering has proved to be an important method for III-V quantum well heterostructure device fabrication, we also review the application of IILD to several different laser diode structures, as well as to passive waveguides. We mention that it may be possible to realize even more advanced device structures using IILD, for example, quantum well wires or quantum well boxes. These will require an even greater understanding of the mechanisms (crystal processes) that control IILD, as well as require more refined methods of pattern definition, masking procedures, and crystal processing.

TABLE OF CONTENTS

I. INTRODUCTION

Since the discovery of impurity-induced layer disordering (IILD) in 1980 by Laidig *et al.*[1] in an attempt to modify undoped $Al_xGa_{1-x}As$-GaAs superlattices (SLs) to doped SLs (for phonon experiments),[2] there has been a growing research effort to understand disordering mechanisms, to understand the crystal and defect diffusion processes inherent in layer disordering, and to utilize the IILD process for device fabrication. Laidig *et al.*[1] found that the layers of an AlAs-GaAs superlattice (SL) are unstable against Zn diffusion and intermix, thus yielding bulk, undamaged, homogeneous material of an Al composition average to that of the original SL. This process occurs at temperatures much less than those necessary for ordinary thermal interdiffusion of the layers of an undoped SL,[3] which, of course, makes IILD especially interesting and important. Since the Zn diffusion can easily be masked at the crystal surface, as in Fig. 1, the impurity-induced layer disordering allows desired regions of quantum well heterostructures (QWHs) to be altered in effective energy gap and refractive index.[4] Figure 2 shows the energy shift directly (in this case a visual color shift) for selective IILD via Si diffusion in an $Al_{0.6}Ga_{0.4}As$-GaAs SL.[5] The IILD is performed in a dot pattern, as might be important in forming an array of quantum well (QW) "dots," and visible spectrum light is transmitted through disordered portions of the crystal. Regions where IILD has shifted the effective energy gap to higher energies appear red, a true color shift, while other areas of the crystal appear dark due to QW band-to-band absorption of the visible spectrum light in the intact SL.

Based on the results of Ref. 1, it was appreciated immediately that impurity implantation, specifically Si implantation (with subsequent annealing of damage), could be used to intermix $Al_xGa_{1-x}As$-GaAs heteroboundaries and layers.[6] Besides the success of Si implantation,[6,7] Camras *et al.*[8] showed that the Zn impurity also could cause disordering when implanted into an $Al_xGa_{1-x}As$-GaAs SL that is then annealed to remove damage. Since this early work,[1-8] many different methods and impurities (or defects) have been found to effect IILD and the selective intermixing of III-V QWHs or SLs. Several different impurities such as the donors Si,[5,9] Ge,[10] S,[11] Sn,[12] and Se,[13] as well as the acceptors Zn,[1] Be,[14] and Mg,[13] have been found to cause layer intermixing either when diffused into the QWH, or during post-growth annealing for the case when the impurities are grown into the crystal. Gavrilovic *et al.*[15] showed that layer intermixing could result from the annealing of lattice damage due to ion implantation. The ion implantation of many different atomic species (not necessarily dopants)[6] has been found to induce layer intermixing.[15-18] In addition, Epler *et al.*[19] have shown that laser melting can be used to incorporate (selectively) Si to a shallow depth in an $Al_xGa_{1-x}As$-GaAs

 0021-8979/88/240R93-21$02.40

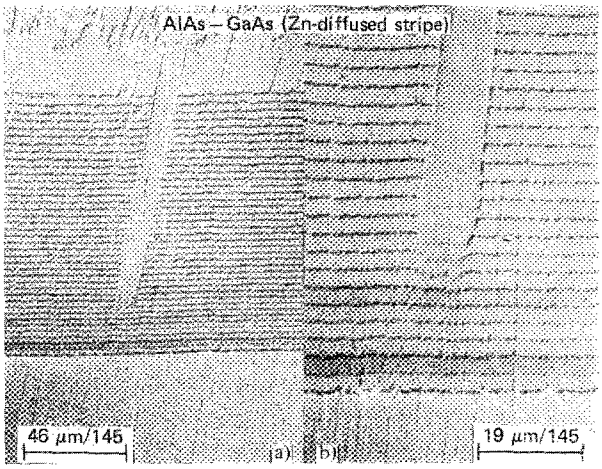

FIG. 1. Shallow-angle ($\sim 0.4°$) cross section of a portion of an AlAs-GaAs superlattice (SL) wafer that, except for a ~ 10-μm stripe, has been masked with Si_3N_4 and has been Zn diffused ($ZnAs_2$) for 10 min at 575 °C. The shallow-angle magnification is $\sim 145\times$ in the vertical direction (no horizontal magnification) and is skewed somewhat relative to the orientation of the Zn-diffused stripe. In the region of the Zn diffusion the 40-period superlattice ($L_z \sim 45$ Å, $L_B \sim 150$ Å) has become compositionally disordered indirect gap $x \sim 0.77$ $Al_xGa_{1-x}As$. (From Ref. 1.)

QWH, and then be used as a diffusion source for IILD.

Studies of IILD have yielded much new information on processes fundamental to the behavior of III-V crystals, for example, self-diffusion, impurity diffusion, and native defect behavior, particularly in regard to control of Column III diffusion in the $Al_xGa_{1-x}As$-GaAs crystal system. In this paper, we review the status of IILD in $Al_xGa_{1-x}As$-GaAs QWHs, and in some related III-V crystals, along with the application of IILD to device fabrication. We also consider

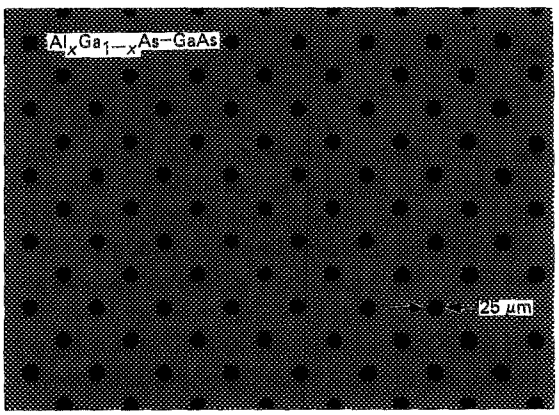

FIG. 2. Dot pattern formed by Si diffusion and layer intermixing of an $Al_xGa_{1-x}As$-GaAs SL. The substrate and buffer layer are removed and the sample is viewed by the portion of white light transmitted upward through the sample. The dark dots are the undiffused SL, and the red regions are the higher gap $Al_{x'}Ga_{1-x'}As$ ($x' \gtrsim 0.32$) formed by the impurity-induced layer disordering (Si IILD).

impurity diffusion mechanisms and their role in IILD in these crystal systems.

II. DISORDERING MECHANISMS IN $Al_xGa_{1-x}As$-GaAs QWHS

The IILD of $Al_xGa_{1-x}As$-GaAs QWHs occurs because of the effect of large impurity concentrations in greatly increasing the Al and Ga self-diffusion rate in the crystal. The crystal self-diffusion rate in QWHs is easily measured by a number of characterization techniques that are sensitive to changes occurring at the heterointerfaces. These include Auger electron profiling,[3] x-ray diffraction,[20] photoluminescence,[21,22] secondary ion mass spectroscopy (SIMS), and transmission electron microscopy (TEM).[23] Although there have also been several previous studies of self-diffusion rates in GaAs using diffusion of radioactive tracers,[24-28] it has been the recent intensive studies of layer intermixing in $Al_xGa_{1-x}As$-GaAs QWHs, taking into account doping effects, that have yielded the most information on self-diffusion mechanisms in the $Al_xGa_{1-x}As$ system, particularly involving the Column III lattice atoms.

The self-diffusion of Column III lattice atoms must proceed through native defects of the crystal. Therefore, the self-diffusion rate will be dependent on the diffusion rate of the native defects, but since the concentration of native defects is typically much less than the concentration of Column III lattice atoms ($\sim 2\times 10^{22}$ cm^{-3}), the Column III self-diffusion rate will also depend on the concentration of the requisite crystal defects. If we consider, for example, self-diffusion on the Column III sublattice through Column III vacancies, then

$$D_{\mathrm{III}} = f D_{V_{\mathrm{III}}} [V_{\mathrm{III}}], \tag{1}$$

where D_{III} is the Column III lattice atom diffusion rate, $D_{V_{\mathrm{III}}}$ is the Column III vacancy diffusion rate, V_{III} is a Column III vacancy, the brackets [ ] denote concentration, and f contains information about the crystal structure[29] and the concentration of Column III lattice sites. Equation (1) shows that as $[V_{\mathrm{III}}]$ increases so will D_{III}. It has been known for a long time that if the point defects in a semiconductor possess various charge states, the equilibrium defect concentrations will depend on the crystal Fermi level.[30] In 1952, Reiss[31] considered the effect of the crystal Fermi level on the solubility of donor and acceptor impurities in a semiconductor, and in 1955 Longini and Greene[32] considered the role of the Fermi level in determining solubilities of both donors and acceptors and the equilibrium concentration of ionized lattice vacancies. In 1960, Shockley and Moll[33] considered the solubility of a general defect with multiple ionized states.

Based on this interaction, Tan and Gösele[34] have suggested that the equilibrium concentration of point defects in III-V crystals depends only on the crystal Fermi level, much as in the case of elemental semiconductors such as Si or Ge. By assuming that both Column III and Column V vacancies can be charged either positively or negatively, Tan and Gösele[34] have suggested that in the case of p-type doping, Column III self-diffusion proceeds mainly because of positively charged Column III vacancies, while Column V diffusion

proceeds because of positively charged Column V vacancies. Similarly, in the case of *n*-type doping Column III self-diffusion proceeds via negatively charged Column III vacancies and Column V diffusion via negatively charged Column V vacancies. Independently, at about the same time, Deppe *et al.*[35] presented data showing that the diffusion of the Si impurity in GaAs is controlled in part by the crystal Fermi energy. Based on the dependence of the Si diffusion rate on the Fermi level and on the As vapor pressure over the crystal during annealing, Deppe *et al.* suggested that the Si diffusion, and the layer intermixing in $Al_xGa_{1-x}As$-GaAs QWHs or SLs that accompanies the Si diffusion, is due to donor vacancy complexes, Si_{Ga}-V_{Ga}.[35] In related work, Kaliski *et al.*[13] have presented experimental data on annealing of QWHs containing either the donor Se or the acceptor Mg showing that for As-rich annealing conditions the *n*-type QWH undergoes considerable intermixing while the *p*-type QWH remains stable. Under As-poor annealing conditions, the *n*-type QWH remains more stable while the *p*-type QWH undergoes layer intermixing. Based on the fact that the layer intermixing depends on the type of doping (*n* or *p*) and As overpressure, the suggestion has been made that intermixing takes place in *p*-type QWHs under As-poor annealing conditions because of Column III interstitials, while the intermixing that takes place in *n*-type QWHs under As-rich conditions is due to Column III vacancies.[13] Devine *et al.*[36] have independently suggested also that layer disordering via acceptor Be diffusion in an $Al_xGa_{1-x}As$-GaAs SL depends on Column III interstitials. Previously, Willoughby[28] has suggested that interstitials are involved in the disordering of $Al_xGa_{1-x}As$-GaAs SLs via Zn diffusion.

Here, we review a model for IILD of $Al_xGa_{1-x}As$-GaAs QWHs based on both the effect of the crystal surface conditions during annealing and the influence of the crystal Fermi level in controlling native defect concentrations.[37,38] The model is simplistic in that only diffusion under equilibrium defect concentrations is considered. Also, native defects are considered as being neutral or only singly ionized. However, we show that predictions for this model of IILD are in qualitative agreement with a wide scope of experimental data concerning Column III self-diffusion and also impurity diffusion in the $Al_xGa_{1-x}As$-GaAs crystal system.

We consider first the experimental data of Guido *et al.*[39] involving annealing experiments on an undoped QWH. The QWH has been grown using metalorganic chemical vapor deposition (MOCVD) and consists of a single GaAs QW of thickness 130 Å at the center of an $Al_{0.25}Ga_{0.75}As$ waveguide region of thickness $\sim 0.25\ \mu$m. The waveguide region is bounded on either side by undoped $Al_{0.85}Ga_{0.15}As$ confining layers of thickness 1 μm. The upper confining layer is capped by a 0.2 μm GaAs layer. The QWH is undoped except for thin regions near the outer boundaries of the $Al_{0.85}Ga_{0.15}As$ confining layers ($\sim 0.2\ \mu$m) which are doped *n*-type ($n_{Se} \sim 10^{18}$ cm^{-3}). Figure 3(a) shows a TEM cross section of the as-grown QWH. Anneals have been performed in sealed quartz ampoules on several different samples of the QWH crystal in which the anneal temperature and time are held constant at 825 °C and 25 h. However, the As vapor pressure over the crystal during the anneal has been varied by varying the amount of excess elemental As added to the ampoule. From Fig. 3(c) we see that when the crystal undergoes thermal annealing, some self-diffusion of the lattice Al and Ga atoms occurs.[39] The diffusion of Al and Ga atoms across the heterointerfaces of the GaAs QW $Al_xGa_{1-x}As$ barriers alters the well's shape, resulting in a shift of the QW energy levels to higher energies.

As has been previously shown,[21] photoluminescence can be used to measure this energy shift and thus the rate of the Al and Ga self-diffusion during the anneal. Figure 4 shows the experimental results of the energy shift of the GaAs QW because of annealing versus the As vapor pressure over the crystal (lower curve).[39] The upper curve in Fig. 4 shows the corresponding Column III self-diffusion rates calculated from the energy shifts. The curves of Fig. 4 show that there is an As vapor pressure at which the Column III self-

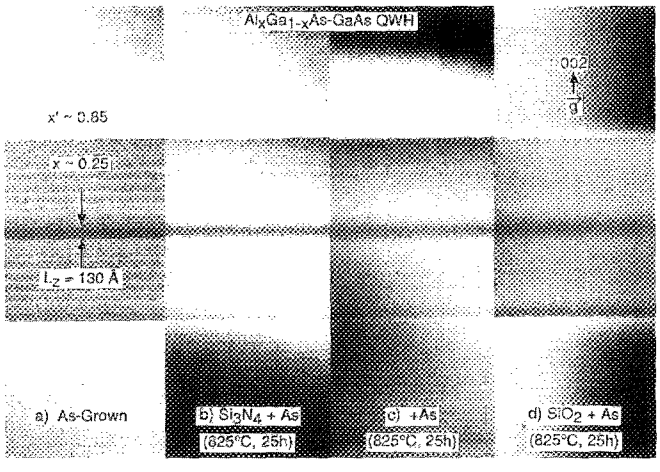

FIG. 3. Cross sections in TEM showing the active region of (a) an as-grown QWH laser crystal, (b) Si_3N_4 capped and annealed sample, (c) capless annealed sample, and (d) SiO_2 capped and annealed sample. The cross sections show that Al-Ga interdiffusion is highly dependent upon the sample encapsulation conditions. (From Ref. 39.)

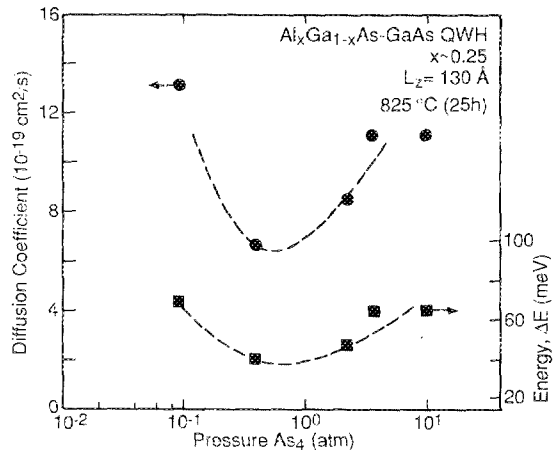

FIG. 4. Measured values of QWH photoluminescence energy shift (relative to the as-grown $Al_xGa_{1-x}As$-GaAs QWH crystal), and the corresponding calculated values of $D_{Al\text{-}Ga}$ as a function of As_4 overpressure. The anneal schedule is fixed (825 °C, 25 h) and the As_4 overpressure is varied by adding As to the anneal ampoules. (From Ref. 39.)

diffusion is a minimum. As the As vapor pressure is increased from this value, the Al-Ga self-diffusion rates increase. Also, as the As vapor pressure decreases from this value, again the Al-Ga self-diffusion rates increase. The shape of the curves for the Al-Ga self-diffusion rate versus As vapor pressure has been further verified in the experimental data of Furuya *et al.*[40]

The diffusion rates of the Column III lattice atoms are sensitive to the As vapor pressure because the diffusion proceeds through native defects, which in concentration are sensitive to the stoichiometry of the III-V crystal. When annealed, the crystal will move toward equilibrium with the surrounding As vapor through either the annihilation or the creation of native defects at the crystal surface. Therefore, defect concentrations near the crystal surfaces (in this case within a few microns) can be shifted through the diffusion of the defects, either from or to the surface, which are mobile at the annealing temperature. It is the diffusion of the mobile defects, and their concentration, that controls the diffusion of the lattice constituents. As the As vapor pressure is increased to larger values in the annealing experiments of Guido *et al.*[39] the crystal stoichiometry is shifted to As-rich and so we expect As-rich defects to control the Al and Ga self-diffusion. The As-rich point defects are the As interstitial, As_I, the As antisite defect, As_{III}, and the Column III vacancy, V_{III}. As the As vapor pressure is decreased below the value at which the Al-Ga diffusion rate is a minimum, we expect As-poor defects to control the diffusion. These are the Al or Ga interstitial, Al_I or Ga_I, the Column III antisite defect, or the As vacancy. We consider the Column III self-diffusion as being due to the Column III vacancy under As-rich annealing conditions, or the Column III interstitial for As-poor conditions.[13,37,38] This interpretation is consistent with both doping effects in the QWHs and impurity diffusion in these crystals.

Figure 5 shows an illustration of a GaAs crystal under an ambient of As_4 vapor. If Frenkel defects can occur in the crystal on the Column III sublattice, we will have the following reaction in the crystal

$$0 \rightleftarrows I_{Ga} + V_{Ga} \quad \text{and} \quad [I_{Ga}][V_{Ga}] = k_1, \tag{2}$$

where k_1 is a constant that depends on temperature and we have used the law of mass action. Because the III-V crystal has a relatively open lattice we expect the I_{Ga} to have a very fast diffusion rate. The interstitial I_{Ga} then can easily diffuse to the crystal surface, where in Fig. 5 we show such a defect diffusing to a step at the crystal surface. (Note that Fig. 5 is not representative of the true GaAs crystal structure, but simply serves as a schematic illustration of the relevant crystal mechanisms.) If there is a large As vapor pressure over the crystal, there is a high probability for an As atom from the vapor to bond at the Ga-rich step, essentially locking what was originally an I_{Ga} defect into a site at the crystal surface. In this manner when the GaAs crystal is annealed under a large As vapor pressure, the crystal surface can act as a sink for Column III interstitial defects, thus increasing the concentration of Column III vacancies deeper in the crystal. Likewise, under As-poor annealing conditions, As will evaporate from the crystal, leaving a Ga-rich surface.

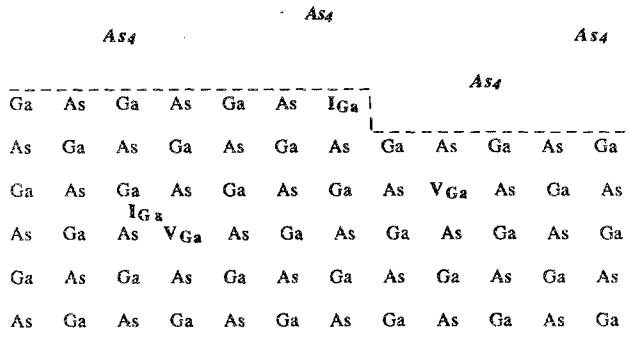

FIG. 5. Schematic illustration of Frenkel defects created in GaAs near the crystal surface. Interstitial defects can react with the As vapor at the crystal surface, thus determining equilibrium defect concentrations in the crystal bulk.

The excess Ga atoms can then diffuse into the crystal increasing the Column III interstitial defect concentration. These reactions can be written as

$$0 \rightleftarrows \tfrac{1}{4}As_4(\text{vapor}) + I_{Ga}, \text{ or } [I_{Ga}] = k_2 P_{As_4}^{-1/4}, \tag{3}$$

where P_{As_4} is the As vapor pressure in the ampoule.

Either the Column III vacancy or the Column III interstitial can lead to Al-Ga self-diffusion by an interaction with Frenkel pair defects. First, we consider the diffusion of the Column III vacancy on its own sublattice. This is illustrated in Fig. 6 for what is initially a V_{Ga} at a GaAs-AlAs heterointerface. The following expression illustrates the vacancy diffusion

$$V_{Ga} \rightleftarrows V_{Ga} + (I_{Al} + V_{Al}) \rightleftarrows (V_{Ga} + I_{Al}) + V_{Al} \rightleftarrows V_{Al}. \tag{4}$$

For the vacancy to diffuse in this manner requires that a lattice atom must move through an interstitial position. Van Vechten[41,42] has suggested that the favored mode for single vacancy diffusion in III-V crystals is through nearest-neighbor hopping. However, he has also shown that in order that a trail of antisite defects not be generated due to the vacancy diffusion, an eleven-step process is required for the vacancy to make one hop on its own sublattice.[42] On the other hand, Vorob'ev *et al.*[43] have suggested that diffusion on its own sublattice will be the favored mode for a vacancy in III-V

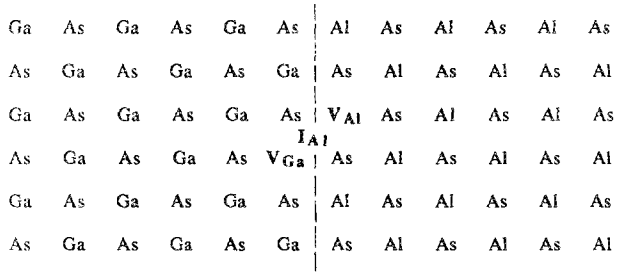

FIG. 6. Schematic illustration of the Column III vacancy migration on the Column III sublattice at an AlAs-GaAs heterointerface. The vacancy diffusion provides a mechanism for Column III self-diffusion and thus AlAs-GaAs interdiffusion. (An Al atom moves from its original lattice site through an interstitial position and into the V_{Ga}.)

crystals. Note that for a diffusion mechanism involving divacancies (V_{III}–V_{As}) we would expect the interdiffusion of the SL layers to be independent of the As vapor pressure, or at most, if one sublattice vacancy tends to always be in excess, the interdiffusion rate may show a continual increase with changing As vapor pressure. However, given the "V" shaped dependence of the Column III self-diffusion rate versus As vapor pressure (Fig. 4)[39] a divacancy process seems unlikely.

The diffusion of the Column III vacancy on its own sublattice suggests that a similar mechanism involving close Frenkel pairs (i.e., V_{Ga}-I_{Ga}) is possible for the diffusion of Column III interstitials.[37,38] This is illustrated in Fig. 7, again for a GaAs-AlAs heterojunction. The Column III interstitial is expected to have a fast diffusion rate through interstitial sites. However, if it encounters, or possibly creates a Frenkel pair, it can move into the Column III vacancy, leaving the original lattice atom free to diffuse away as an interstitial defect and repeat the interaction at some distant site. We can describe this in the reaction

$$I_{Ga} \rightleftarrows I_{Ga} + (V_{Al} + I_{Al}) \rightleftarrows (I_{Ga} + V_{Al}) + I_{Al} \rightleftarrows I_{Al}. \quad (5)$$

Now if we consider the effect of both Column III vacancies and Column III interstitials on the Column III self-diffusion rate, we obtain an expression given by

$$D_{III} = f_1 D_{V_{III}} [V_{III}] + f_2 D_{I_{III}} [I_{III}]. \quad (6)$$

And, if we substitute into Eq. (6), Eqs. (2) and (3), we obtain

$$D_{III} = f_1' D_{V_{III}} P_{As_4}^{1/4} + f_2' D_{I_{III}} P_{As_4}^{-1/4}. \quad (7)$$

It can be seen that Eq. (7) does indeed describe the trend shown earlier in Fig. 4.[39] As the As vapor pressure increases to give As-rich annealing conditions, we expect D_{III} to increase due to the Column III vacancies. As the As vapor pressure decreases to give As-poor annealing conditions, we expect D_{III} to increase due to Column III interstitials, and at some intermediate As vapor pressure we expect D_{III} to go through a minimum, as can be seen in Fig. 4. At this point we note that a similar expression to Eq. (7) can be obtained by assuming some form of diffusion mechanism for Column III lattice atoms involving Column V vacancies. However, it is not necessary to identify or construct such a diffusion mechanism because the assumption of Column III vacancies and Column III interstitials as the important native defects for Column III self-diffusion provides a sufficient basis to explain a wide variety of experimental data for both self-diffusion and impurity diffusion in III-V materials, particularly for IILD via Zn diffusion.

Also we mention here that although the Column III self-diffusion due to both the Column III vacancy and the Column III interstitial involve the close Frenkel pair, V_{III}–I_{III}, the two diffusion mechanisms may not have similar activation energies. The diffusion due to either mechanism depends on diffusion of the defect itself, which will undoubtedly have different activation energies for either V_{III} or I_{III}. But also the creation of the Frenkel pair must occur in the *presence* of either point defect, either the V_{III} or I_{III}, for Column III self-diffusion to occur. The presence of either point defect in the crystal may have a large and different influence on the activation energy for the creation of the Frenkel pairs.

Although the previous discussion has concerned undoped QWHs in which the background impurities are expected to have only a minor effect, it has been shown that when a large concentration of impurities is present in the crystal, the Al-Ga self-diffusion rate can be increased by orders of magnitude.[1] For example, Fig. 8 shows data of Mechan *et al.*[5] of a TEM cross section of an $Al_{0.5}Ga_{0.5}As$-GaAs SL in which the SL region on the left has been Si diffused while on the right the crystal has been masked at the surface to block the Si diffusion. Where the crystal has been Si diffused the Al-Ga self-diffusion (or interdiffusion) rate has increased to the extent that the SL layers have become completely intermixed. The Si impurity acts predominantly as a donor when diffused into $Al_xGa_{1-x}As$ or GaAs and so will greatly increase the electron concentration in the diffused regions. As stated earlier, the shift in the Fermi level that accompanies the Si diffusion can have a large effect on equilibrium defect concentrations in those regions, if the defects possess charge states.[31–35] For a formal treatment of the interaction in a semiconductor between the crystal Fermi level

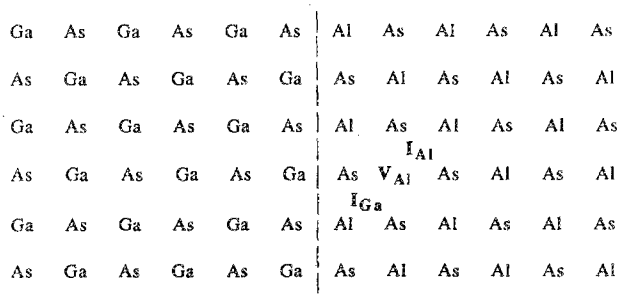

FIG. 7. Schematic illustration of the Column III self-diffusion through a Column III interstitial mechanism. The interstitial mechanism can lead to layer interdiffusion at the AlAs-GaAs heterointerface through a reaction with the V_{Al}-I_{Al} Frenkel pair.

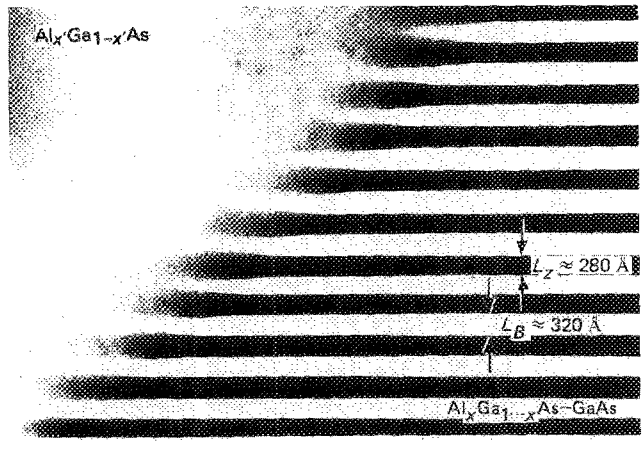

FIG. 8. Bright field transmission electron microscope (TEM) micrograph of a 40-period $Al_xGa_{1-x}As$-GaAs superlattice ($x \gtrsim 0.6$, $L_B \approx 320$ Å, $L_z \approx 280$ Å) that on the left-hand side has been disordered into bulk crystal $Al_{x'}Ga_{1-x'}As$ by Si diffusion and on the right-hand side is masked (Si_3N_4 protected) as-grown SL that has "survived" the 850 °C (10 h) anneal cycle. (From Ref. 5.)

and charged defects, the reader is referred to Ref. 32. Here we consider the simplified case of n-type GaAs crystal containing a fixed amount of donor impurities.

Of the six point defects possible in GaAs or $Al_xGa_{1-x}As$, only the Column III vacancy, V_{III}, and the Column III antisite defect, Al_{As} or Ga_{As}, are expected to have acceptorlike energy states in the crystal.[44,45] The other four are expected to act as donor-type defects.[45] Since the V_{III} is expected to play a major role in Column III self-diffusion, we consider the equilibrium concentration of this defect in more detail. We consider first, the case in which the GaAs crystal is annealed in a sealed ampoule under As-rich conditions, and all V_{III} defects created are in a neutral state. Under these conditions the free energy of the crystal can be expressed as[46]

$$F(\text{crystal}) = F_o + N_v^x \Delta U_v - k_B T \ln[N_l!/(N_l - N_v^x)!N_v^x!], \quad (8)$$

where N_v^x is the number of neutral Column III vacancies in the crystal ("x" designating neutral configuration), N_l is the number of Column III lattice sites, T is the annealing temperature, ΔU_v is the energy increase of the crystal upon creation of a vacancy, k_B is Boltzmann's constant, and F_0 is that part of the crystal free energy independent of N_v^x. Here, we have neglected surface effects.[47] If we treat the As vapor in the ampoule as an ideal gas of As_4 molecules, its free energy can be written as[48]

$$F(\text{vapor}) = (N_{As}/4)k_B T\{\ln[(N_{As}/4V) \times (2\pi\hbar^2/Mk_B T)^{3/2}] - 1\}, \quad (9)$$

where N_{As} is the number of As atoms in the vapor, V is the volume of the ampoule, $\hbar$ is Planck's constant, and M is the mass of an As_4 molecule. If we assume that with the creation of every Column III vacancy we remove $\frac{1}{4}$ of an As_4 molecule from the vapor, we can minimize the free energy of the total system (crystal + vapor) with respect to the number of Column III vacancies, N_v^x. This gives the equilibrium concentration of Column III vacancies in the GaAs as

$$[V_{III}^x] \approx C P_{As_4}^{1/4} (2\times 10^{22}) \exp(-\Delta U_v/k_B T)\,\text{cm}^{-3}, \quad (10)$$

where C is a constant depending on temperature. Although essentially the same result can be found using the law of mass action, Eqs. (2) and (3), Eq. (10) has the virtue of also giving the dependence of $[V_{III}^x]$ on ΔU_v, the energy cost for the crystal to create a vacancy. Now, if the Column III vacancies have an acceptor level and in n-type material become charged,[44,45] we must also consider the free energy of the electronic system[32] in the crystal. If we assume that the crystal is strongly n-type and the crystal Fermi level is far enough in energy above the vacancy acceptor energy level E_A, most of the Column III vacancies will be ionized as illustrated in Fig. 9. Although it costs the crystal some energy to create the acceptor level, because it must create a Column III vacancy, the crystal loses energy in the ionization of the vacancy by dropping an electron from the conduction band to the vacancy acceptor level.

We consider GaAs doped n-type to a level $\gtrsim 10^{18}\,\text{cm}^{-3}$. The intrinsic carrier concentration in GaAs at an anneal temperature of 800 °C is about $5\times 10^{16}\,\text{cm}^{-3}$.[40] Therefore, under these conditions charge neutrality gives the relation

$$[N_d^+] \approx n + [V_{III}], \quad (11)$$

where $[N_d^+]$ is the donor (impurity) concentration. If we assume that for the n-type doping the number of ionized vacancies is much greater than the number of neutral vacancies, i.e., $N_v^- \gg N_v^x$, we can rewrite the expression for the crystal free energy considering the ionized vacancies as

$$F(\text{crystal}) = F_o' + F_{el}(N_v^-) + N_v^- E_A + N_v^- \Delta U_v - k_B T \ln \frac{N_l!}{(N_l - N_v^-)!N_v^-!}, \quad (12)$$

where $F_{el}(N_v^-)$ is the electronic free energy which now depends on the number of charged vacancies. The total free energy of the crystal and vapor is again easily minimized since, using Eq. (11), $dn = -dN_v^-$. We then have

$$\frac{\partial F_{el}(N_v^-)}{\partial N_v^-} = \frac{-\partial F_{el}}{\partial n} = -E_F. \quad (13)$$

This gives for the equilibrium concentration of ionized vacancies

$$[V_{III}] \approx C_1 P_{As_4}^{1/4} \exp\{-[\Delta U_v - (E_F - E_A)]/(k_B T)\} = [V_{III}^x]\exp[(E_F - E_A)/(k_B T)]. \quad (14)$$

Equation (14) shows that as the Fermi level in the semiconductor is increased (through an increase in donor impurity concentration) the crystal will have an increased solubility for the acceptorlike V_{III} defect.

Similar arguments will hold for the crystal solubility of donorlike defects in a p-type crystal. The donorlike Column III interstitial[44,45] can lose energy by dropping an electron to the crystal Fermi level, which will be close to the valence band for strongly p-type crystal. In this case, the equilibrium concentration of ionized Column III interstitials will be

$$[I_{III}^+] = [I_{III}^x]\exp[(E_D - E_F)/(k_B T)] = C_2 P_{As_4}^{1/4} \exp\{-[\Delta U_I - (E_D - E_F)]/(k_B T)\}. \quad (15)$$

Vacancies (V_{III}^-) in n+ III-V Semiconductor

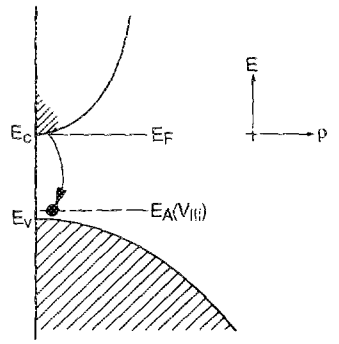

FIG. 9. Ionization of a Column III vacancy acceptor level in an n-type III-V crystal. Although there is an energy cost for the crystal to create the vacancy and corresponding acceptor level, the crystal loses energy by dropping an electron from the conduction band to the vacancy acceptor level. This makes the total energy cost for the ionized vacancy in the crystal dependent on the Fermi level.

Using Eq. (6), we obtain a new expression for the Column III self-diffusion rate based on Column III vacancies and Column III interstitials, i.e.,

$$D_{\mathrm{III}} = f_1'' P_{\mathrm{As_4}}^{1/4}\{D_{V_{\mathrm{III}}} + D_{V_{\mathrm{III}}}\exp[(E_F - E_A)/(k_B T)]\} + f_2'' P_{\mathrm{As_4}}^{-1/4}\{D_{I_{\mathrm{III}}} + D_{I_{\mathrm{III}}}\exp[(E_D - E_F)/(k_B T)]\}. \quad (16)$$

Equation (16) shows that in $Al_xGa_{1-x}As$-GaAs the Column III self-diffusion will increase first of all when the crystal is strongly n-type and annealed under As-rich conditions (both effects favoring a high crystal solubility for the Column III vacancy), or when the crystal is strongly p type and annealed under As-poor conditions (both effects favoring a high solubility for Column III interstitials).

This behavior has been previously investigated through anneals performed on $Al_xGa_{1-x}As$-GaAs SLs containing various types of doping impurities.[37,38,50] Figure 10 shows TEM cross sections of a Se-doped $Al_{0.5}Ga_{0.5}As$-GaAs SL in which the measured electron concentration is $\sim 2\times 10^{18}$ cm^{-3}. The SL, along with an undoped SL, has been annealed in sealed quartz ampoules for 10 h at 825 °C with varying As vapor pressures. In all cases, the ampoule volume has been kept fixed at ~ 2.5 cm^3. For the first anneal, shown in Fig. 10(a), elemental Ga is added to the ampoule. At the anneal temperature the Ga acts as a sink for As that evaporates from the crystal surface, thus resulting in a very low As vapor pressure during the anneal. This annealing condition is extremely As-poor. In the second anneal, shown in Fig. 10(b), the crystals are annealed by themselves in the ampoule. In this case, the crystals lose a small amount of As to the vapor until an equilibrium As vapor pressure with the crystals is reached. These also are As-poor annealing conditions, however, much less so than in the anneal of Fig. 10(a). For the third anneal, ~ 30 mg of elemental As is added to the ampoule, corresponding to very As-rich conditions. After all three anneals, both the Se-doped and the undoped SLs have been studied using shallow angle beveling. The crystals are then stained with an etch that is sensitive to composition and are examined under an optical microscope. Based on this technique, the layers of the undoped SL have been found to be stable under all three annealing conditions. For the Se-doped SL the shallow angle bevel reveals layer intermixing consistent with the TEM data of Fig. 10. Under extremely As-poor annealing conditions, Fig. 10(a), the layers of the SL remain stable, i.e., the Al-Ga self-diffusion rate is small. As the annealing conditions are made less As-poor, Fig. 10(b), the Column III self-diffusion increases and the layers of the Se-doped SL partially intermix. Under As-rich annealing conditions, Fig. 10(c), the Al-Ga diffusion rate is fast, and complete layer intermixing occurs in the donor doped SL.

An $Al_{0.4}Ga_{0.6}As$-GaAs SL doped with the donor Si (giving a measured electron concentration of 10^{18} cm^{-3}) has also been investigated.[37,38] Transmission electron microscope cross sections of this SL are shown in Fig. 11. Figure 11(a) shows the "as-grown" SL, which can be seen to have sharp heterointerfaces. When the crystal is annealed under As-poor conditions, Fig. 11(b), some Al-Ga self-diffusion occurs, but the layers of the SL remain intact. When the SL is annealed under As-rich conditions, Fig. 11(c), the layer interdiffusion of the SL increases significantly. Therefore, the same trend is found in the Si-doped SL as in the Se-doped case. Specifically, in n-type crystal the SL layers intermix under As-rich annealing conditions. Both the donor doping and As-rich annealing conditions favor a high concentration of Column III vacancies and, hence, layer intermixing. In contrast, the SL layers are more stable under As-poor annealing conditions.

The effect of p-type doping (Mg doping) has also been investigated.[38] Figure 12 shows TEM cross sections of a Mg-doped $Al_{0.4}Ga_{0.6}As$-GaAs SL with a measured hole concentration of 8×10^{18} cm^{-3}. Figure 12(a) shows the SL immediately after crystal growth, and again it can be seen that the heterointerfaces are relatively sharp. However, when the SL is annealed under As-poor conditions (sample alone in a sealed quartz ampoule), Fig. 12(b), the layers of the SL are found to intermix (high Al-Ga self-diffusion rate). When

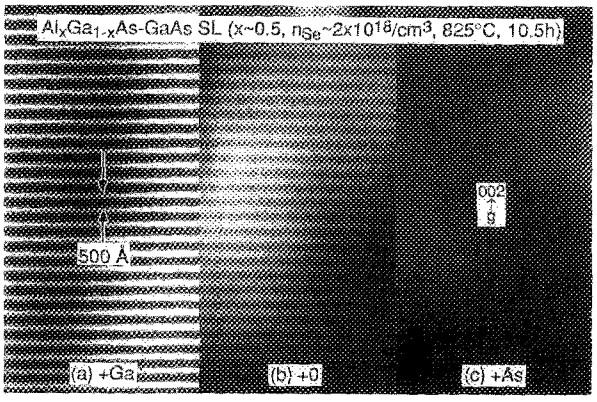

FIG. 10. TEM image of a Se-doped SL after annealing in different environments: (a) Shows little layer intermixing upon annealing under Ga-rich conditions, while (b) shows increased layer intermixing when the SL is annealed in an evacuated ampoule. When the SL is annealed under As-rich conditions, (c) almost complete layer intermixing occurs. (From Ref. 50.)

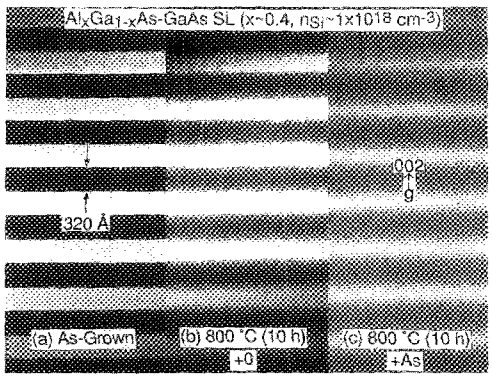

FIG. 11. Transmission electron microscope images of the cross sections of a Si-doped ($n_{\mathrm{Si}} \sim 10^{18}$ cm^{-3}) $Al_{0.4}Ga_{0.6}As$-GaAs SL for (a) the as-grown crystal, (b) after annealing at 800 °C (10 h) under As-poor conditions, and (c) after annealing at 800 °C (10 h) under As-rich conditions. The layer interdiffusion in the SL is enhanced under (c) As-rich annealing conditions. (From Ref. 38.)

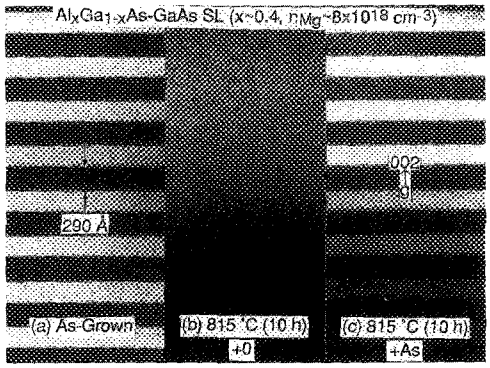

FIG. 12. Transmission electron microscope image of cross sections of a Mg-doped ($n_{Mg} \sim 8\times10^{18}$ cm^{-3}) $Al_{0.4}Ga_{0.6}As$-GaAs SL for (a) the as-grown crystal, (b) after annealing at 815 °C (10 h) under As-poor conditions, and (c) after annealing at 815 °C (10 h) under As-rich conditions. Contrary to the Si-doped SL of Fig. 11, the layer interdiffusion in the Mg-doped SL is enhanced under (b) As-poor annealing conditions, not (c) As-rich conditions. (From Ref. 38.)

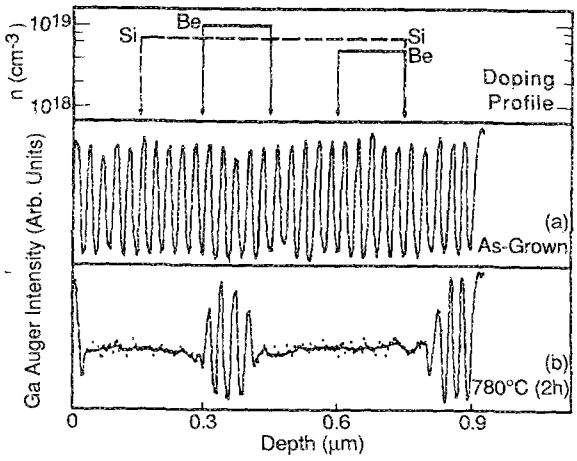

FIG. 13. Auger profile of Ga in an AlAs-GaAs SL containing Si and Be impurities for (a) the as-grown crystal and (b) after annealing at 780 °C (2 h). (From Kawabe *et al.* Ref. 51.)

annealed under As-rich conditions, Fig. 12(c), the *p*-type SL is found to be stable. This behavior is in direct contrast to that of *n*-type SLs. In the case of the *p*-type SL, both the acceptor doping and the As-poor annealing conditions favor a high concentration of Column III interstitials, which leads to a large Column III self-diffusion rate.

It has been suggested[40] that the "V" shaped dependence of the Column III self-diffusion on the As vapor pressure, i.e., Fig. 4, is due to the III-V crystal's ability to convert a Column V vacancy into a Column III vacancy through the reaction

$$V_{As} \rightleftarrows Ga_{As} + V_{Ga}. \tag{17}$$

The Column III self-diffusion would then be due to Column III vacancies under both As-rich and As-poor annealing conditions. This mechanism is inconsistent with the trends found in the doped SLs.[37,38,50] Both the Ga_{As} antisite defect and the V_{Ga} vacancy are expected to act as acceptors.[44,45] Thus, if reaction Eq. (17) were to occur, it would heavily favor the creation of both the Ga_{As} antisite defect and V_{Ga} vacancy in *n*-type crystal under As-poor annealing. However, Fig. 10(a) shows that as the annealing conditions become more As-poor, the *n*-type SL becomes more stable. Also, reaction (17) offers no explanation for the data presented in Fig. 12 for a *p*-type SL, all of which points to the importance and influence of the Fermi-level location and to the Column III interstitial defect.

The strong influence of the crystal Fermi level (its position) has also been shown directly in other experiments involving the doping of QWHs with both donor and acceptor impurities.[12,13,51] We see clearly from the experimental data of Kawabe *et al.*[51] shown in Fig. 13, the importance of the crystal Fermi level (and not simply the impurity concentration) in controlling layer intermixing. These workers in their studies have used an AlAs-GaAs SL uniformly doped with the Si impurity to a concentration of 7×10^{18} cm^{-3} and in selected regions counterdoped with the acceptor Be as shown in Fig. 13 (upper panel). Using Auger electron profiling, they have found (after sample annealing at 780 °C, 2 h, Fig. 13b), that where the Si exceeds the Be concentration (and the crystal is *n* type), the SL layers intermix. Where the Be concentration exceeds that of the Si and the crystal is converted to *p* type, the SL remains stable. Although the effect of the Fermi level was not pointed out in that study,[51] the experimental data are consistent with the arguments discussed above concerning the importance of the Fermi level and its position.

In considering the effect of the crystal Fermi level on equilibrium concentrations of charge defects, we have considered only singly ionized states. The occurrence of doubly or possibly triply ionized states for Column III vacancy or interstitial defects[45] would increase the dependence of the defect concentration on the crystal Fermi level.[33,34] However, the ionization energy levels for the native defects of III-V crystals have been difficult to measure experimentally and are uncertain. Also, the ionization energy levels of defects such as vacancies may have a strong temperature dependence,[52] which would reduce the usefulness of room-temperature measurements.

Further, to the issue of the effect of the crystal Fermi level, Mei *et al.*[53] have studied the dependence of the Al-Ga diffusion as a function of the concentration of a grown-in Si impurity source. They have found, for $Al_xGa_{1-x}As$, that the Al self-diffusion rate shows a power law dependence on the Si concentration.[53] Figure 14 shows plots of the measured Al diffusion rate versus temperature for several different Si concentrations.[53] The highest concentration of Si used was 5×10^{18} cm^{-3}, above which Si donors present in the crystal typically become compensated. The data of Mei *et al.*[53] show that although the Al diffusion rate in the $Al_xGa_{1-x}As$ crystal is indeed very sensitive to the Si donor concentration present, the activation energy of the diffusion process is relatively unchanged for Si concentrations between 5×10^{17} and 5×10^{18} cm^{-3}. Mei *et al.*[53] have interpreted the data as pointing to a divacancy process controlling the layer intermixing. They have also pointed out, however, that the data are consistent with an increase in the hopping prob-

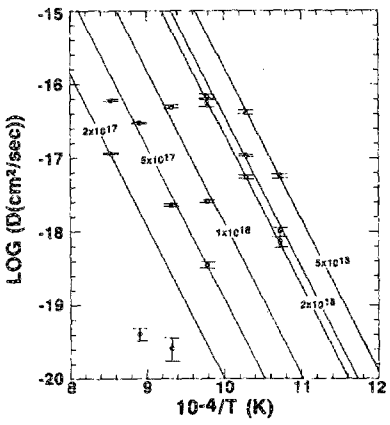

FIG. 14. Arrhenius plots of Al diffusion coefficients at several Si concentration. (From Mei *et al.* Ref. 53.)

ability of the Al atoms (Column III lattice atoms) as opposed to a reduction of a potential barrier impeding the atom hopping.[53] This is consistent with the Column III vacancy mechanism in which the vacancy concentration follows the donor impurity concentration (or Fermi level).

In a recent paper, Tan and Gösele[54] have also concluded that IILD in $Al_xGa_{1-x}As$-GaAs QWHs is due to Column III vacancies in the case of n-type doping and Column III interstitials for p-type doping. Figure 15 shows the dependence of the layer intermixing rate on the impurity concentration for AlAs-GaAs SLs. This plot has been prepared by Tan and Gösele[54] using the experimental data of several workers.[14,16,18,51,53,55,56] The interdiffusion rate for the AlAs-GaAs SL is found to vary with the cube of the Si concentration (Fig. 15, left-hand side). As pointed out by Tan and Gösele,[54] the cubic power dependence points to a triply negatively ionized Column III vacancy, V_{III}^{3-}, as controlling the layer intermixing. On the right-hand side of the figure, data are shown compiled for the acceptor impurities Zn and Be. The large difference in the effect of the two impurities on the layer intermixing is a function of whether the impurity diffuses into the crystal from an external source, as is the case for Zn, or simply is present as a grown-in source, which is the case for Be.[54] This will be discussed further when we consider the diffusion behavior of Zn in Sec. III B.

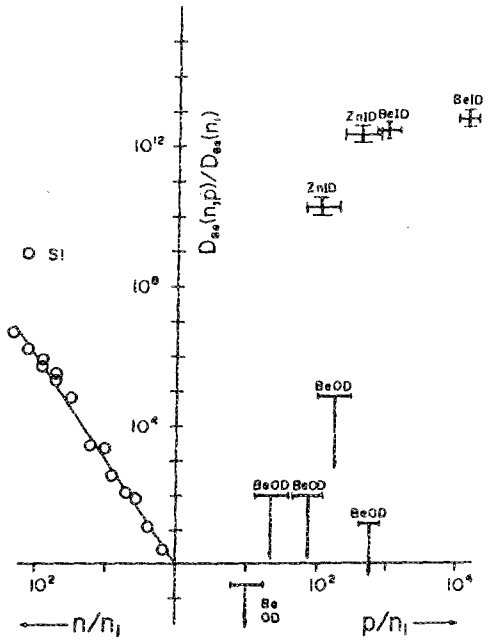

FIG. 15. Plot of normalized Ga diffusion constant $D_{Ga}(n,p)/D_{Ga}(n_i)$. On the left-hand side the data due to Si doping are derived from those of Mei *et al.* (Ref. 53). The $(n/n_i)^3$ dependence is apparent. On the right-hand side, the data due to Zn doping are derived from those of Lee and Laidig (Ref. 55), the data due to Be are estimated from those of Kawabe *et al.* (see Ref. 51), Myers *et al.* (Ref. 56), Hirayama *et al.* (Ref. 18), Ralston *et al.* (Ref. 16), and Kamata *et al.* (Ref. 14). $D_{Ga}(p) = 1\times10^{-19}\,cm^2\,s^{-1}$ as an upper bound is assumed for cases in which no disordering enhancement is observed (Refs. 14, 16, 18, 51, 56). OD and ID denote the out-diffusion and in-diffusion cases, respectively. (From Tan and Gösele, Ref. 54.)

At this point, we consider a bit further the activation energy of the interdiffusion process and how it varies with doping, even though the data on this matter are rather sparse.[53] Although the Al-Ga interdiffusion rate of AlAs-GaAs SLs depends strongly on the Si doping concentration present in the crystal (a cubic dependence as mentioned earlier), Mei *et al.*[53] have also found that the activation energy for the interdiffusion is constant at ~ 4 eV for Si concentrations above $5\times10^{17}\ cm^{-3}$. Tan and Gösele,[54] meanwhile, have shown that if the interdiffusion data of Mei *et al.*[53] are normalized by $(n/n_i)^3$, n being the Si doping concentration and n_i the intrinsic carrier concentration, the interdiffusion rate is consistent with the available self-diffusion data of Ga in undoped GaAs.[54] This has led them[54] to suggest that the triply ionized Column III vacancy, V_{III}^{3-}, is responsible for Column III self-diffusion under both n-type doping and intrinsic conditions. However, the activation energy for the Column III self-diffusion under intrinsic conditions has been measured to be ~ 6 eV.[54] Therefore, it is important to recognize when interpreting these data how the self-diffusion activation energy varies with doping when charged defects are involved.

For example, if we consider the case of n-type doping and the Column III vacancy diffusion process, for multiply ionized defects the diffusion rate can be written as

$$D_{III} = C([V_{III}^{x}]D_{V_{III}^{x}} + [V_{III}^{-}]D_{V_{III}^{-}} + [V_{III}^{2-}]D_{V_{III}^{2-}} + [V_{III}^{3-}]D_{V_{III}^{3-}} + \cdots), \qquad (18)$$

where C is a constant in this case that contains information about the crystal structure. The diffusion rate due to each ionized state of the Column III vacancy will be governed, in general, by a different activation energy. The activation energy for diffusion due to the triply ionized Column III vacancy, for example, will consist of a contribution from the migration enthalpy contained in $D_{V_{III}^{3-}}$ and also a contribution from the formation enthalpy contained in $[V_{III}^{3-}]$. It is important to consider the formation enthalpy of V_{III}^{3-} and its dependence on the doping in the crystal. The concentration of V_{III}^{3-} can be written in terms of $[V_{III}^{x}]$, i.e.,[33]

$$[V_{III}^{3-}] = [V_{III}^{x}]\exp[(3E_F - E_A)/kT], \qquad (19)$$

where E_A is the combined ionization energy (3 electrons)

for the triply ionized vacancy. The neutral Column III vacancy, V_{III}^{x}, will have a formation enthalpy independent of the doping. If the donor concentration is much less than the intrinsic carrier concentration, i.e., $N_d^+ \ll n_i$, then

$$E_F = E_v/2 + kT/2 \ln(N_v/N_c), \tag{20}$$

where E_c is the conduction-band energy, N_v is the effective valence-band density of states, N_c is the effective conduction-band density of states, and the top of the valence band is the zero energy reference. This gives for the concentration of triply ionized vacancies

$$[V_{III}^{3-}] = [V_{III}^{x}](N_v/N_c)^{3/2}\exp[(\tfrac{3}{2}E_c - E_A)/kT]. \tag{21}$$

Although the formation enthalpy for V_{III}^{3-} will have contributions from the formation enthalpy of V_{III}^{x} and the ionization energy, in Eq. (21) we focus on the term that depends on the conduction-band energy, that is $(\frac{3}{2})E_c$, since it is this term that is affected most by changing the doping from intrinsic to extrinsic. For the case of n-type doping when $n \approx N_d^+ \gg n_i$, the Fermi energy level becomes

$$E_F = E_c + kT \ln(N_d^+/N_c), \tag{22}$$

and the concentration of triply ionized Column III vacancies becomes

$$[V_{III}^{3-}] = [V_{III}^{x}](N_d^+/N_c)^3\exp[(3E_c - E_A/kT)]. \tag{23}$$

Therefore, even though a triply ionized Column III vacancy, V_{III}^{3-}, may control the self-diffusion under both intrinsic and n-type doping, the activation energy for the diffusion process will be reduced by $(\frac{3}{2})E_c$ for intrinsic to n-type doping conditions. Of course, if different charge states of the defect become important under different doping conditions, changes will also occur in the measured activation energy due to changes in the migration enthalpy as well as changes in the formation energy.

III. IMPURITY DIFFUSION IN $Al_xGa_{1-x}As$-GaAs AND RELATED III-V CRYSTALS

A. Si diffusion

Silicon diffusion in GaAs and $Al_xGa_{1-x}As$ has been the topic of several studies.[5,35,38,57-66] Vieland[57] and Antell[58] have shown that the Si diffusion rate into GaAs (which is the often studied prototype case) from an elemental source deposited on the crystal, is a strong function of the As vapor pressure over the crystal. The diffusion rate is found to increase with the As vapor pressure, and if no As vapor pressure is supplied to the crystal, the Si diffusion rate goes to zero.[58] The diffused layers are highly doped n type but are also extremely compensated.[58,59] Greiner and Gibbons[59] have shown using secondary ions mass spectroscopy (SIMS) that the Si diffusion rate is concentration dependent, and based on this and the high degree of compensation have suggested that the Si diffuses as neutral pairs Si_{Ga}-Si_{As}. Deppe *et al.*[35,66] however, have shown that the Si diffusion rate is not simply concentration dependent, but dependent on the crystal Fermi level. Because of the dependence on both the As vapor pressure and the Fermi level, they have suggested instead, that the Si diffuses as donors on the Column III sublattice employing Column III vacancies.[35,66] Here, we review the diffusion of Si in GaAs through Column III vacancies and show that this mechanism is consistent with experimental data concerning both Si diffusion and IILD in $Al_xGa_{1-x}As$-GaAs QWHs.[5]

We consider the case in which the Si is diffused into undoped GaAs. As the Si diffuses it converts the GaAs to strongly n-type material. This will increase the probability for acceptorlike defects such as the Column III vacancy to be in a negatively charged state.[44,45] Since the Si_{Ga}^+ donor is in a positively charged state there will be a binding energy for the two to exist as a complex, $Si_{III}^+ - V_{III}^-$. As in earlier discussions, we consider in detail only the singly ionized Column III vacancy, although other charge states may indeed be more important.[53,54] This reaction takes place in the crystal as

$$Si_{III}^+ + V_{III}^- \rightleftarrows (Si_{III} - V_{III}),$$

and

$$[Si_{III} - V_{III}] = K_3[Si_{III}^+][V_{III}^-]. \tag{24}$$

Under the assumption that the V_{III} defect can diffuse on its own sublattice, the $Si_{III} - V_{III}$ complex will also be free to diffuse,[35] while the Si_{III}^+ isolated donor will be immobile. The diffusion of the Si impurity will then be controlled by the diffusion and concentration of the Column III vacancy. For the Si diffusion rate, therefore, we will have

$$D_{Si} = D_{Si_{III}-V_{III}}\partial[Si_{III} - V_{III}]/\partial[Si]. \tag{25}$$

The ionization of the Column III vacancy can be expressed as

$$V_{III}^{x} + e^- \rightleftarrows V_{III}^-, \text{ and } [V_{III}^-] = K_4 n[V_{III}^{x}]. \tag{26}$$

Using Eqs. (2) and (3), we can express $[V_{III}^{x}]$ as a function of the As vapor pressure. For a diffusion temperature of 800 °C the intrinsic carrier concentration is about 5×10^{16} cm^{-3}.[49] Thus, if the electron concentration is above $\sim5\times10^{17}$, the charge neutrality condition governing the crystal can be written as

$$[Si_{III}^+] \approx n + [V_{III}^-]. \tag{27}$$

Although we will discuss in more detail experimental data concerning the binding energy of the $Si_{III} - V_{III}$ complex, for the present argument we consider the complex as being only weakly bound. Under the conditions of a small binding energy for the $Si_{III} - V_{III}$ complex and a significant diffusion rate for the V_{III} defect, we assume $[Si_{III}^+] \gg [Si_{III} - V_{III}]$ so that for the total concentration of Si,

$$[Si] = [Si_{III}^+] + [Si_{III} - V_{III}] \approx [Si_{III}^+]. \tag{28}$$

Using Eqs. (2), (3), (24), and (26)–(28), we can write the concentration of the $Si_{III} - V_{III}$ complexes as a function of the total Si concentration and As vapor pressure, i.e.,

$$[Si_{III} - V_{III}] = k_3\frac{k'P_{As_4}^{1/4}}{1 + k'P_{As_4}^{1/4}}[Si]^2. \tag{29}$$

Equation (29) then gives for the Si diffusion rate from Eq. (25)

$$D_{Si} = D_{Si_{III}-V_{III}}2k_3\frac{k'P_{As_4}^{1/4}}{1 + k'P_{As_4}^{1/4}}[Si], \tag{30}$$

which is a diffusion rate which depends on the Si concentration. This is consistent with the experimental data of Greiner and Gibbons.[59] As in the case of the Column III self-diffusion,[53,54] the Si diffusion rate may show a power law dependence on the Si concentration if the V_{III} vacancy is multiply ionized.

The assumption of $[Si_{III}^{+}] \gg [Si_{III} - V_{III}]$ will be most valid at the Si diffusion front where both the Si concentration and the Column III vacancy concentration are smaller. Note that we have assumed that the Si is diffusing into undoped GaAs. If background impurities are present in the crystal, their effect on the Si diffusion rate will enter into Eq. (30) through the charge neutrality condition, i.e., Eq. (27). Instead of $[Si_{III}^{+}]$ on the left-hand side of Eq. (27) it is necessary to substitute the net concentration of donor impurities. We would expect, therefore, that the Si diffusion rate decreases in p-type crystal because of the reduced concentration of existing vacancies, i.e., Eq. (26), or to be increased in n-type crystal. This behavior has, in fact, been found by Deppe *et al.*[35,66] for both p and n background doping. Figure 16 shows SIMS profiles of Si diffusion into several different GaAs crystals containing various concentrations of the acceptor Zn. To insure identical diffusion conditions, all four wafers have received simultaneous depositions of an elemental Si diffusion source, ~200 Å Si and a 1000 Å SiO_2 cap. The wafers have been diffused in the same ampoule to insure an equal As vapor pressure. As can be seen in Fig. 16, as the Zn concentration increases from 10^{17} cm^{-3}, profile (a), to 10^{20} cm^{-3}, profile (d), the Si diffusion consistently becomes more shallow. The Zn doping of 10^{20} cm^{-3} almost totally blocks the Si diffusion. Figure 17 shows the effect of an n-type dopant, Sn.[66] In this case, we have also included a Zn-doped wafer for reference, profile (a). As the Sn doping increases from 10^{16} cm^{-3}, profile (b), to 3×10^{18} cm^{-3}, profile (c), the Si diffusion is seen to increase. Note also that the shape of the Si diffusion front changes in the more heavily Sn-doped wafer, becoming less abrupt or less dependent on the Si concentration. This occurs because the vacancy concentration at the Si diffusion front is increased by the high level of the donor Sn as compared to being decreased for the p-type wafers.[35,66]

The dependence of the Si diffusion rate on As overpressure has been investigated for GaAs by Vieland,[57] Antell,[58] and for GaAs and $Al_xGa_{1-x}As$ by Guido *et al.*[65] Similar relationships have been found in all three studies for Si diffusion into GaAs and that are consistent with Eq. (30). We show the data of Guido *et al.*[65] in Fig. 18. As the As vapor pressure increases, the concentration of ionized Column III vacancies, determined by the net donor concentration in the

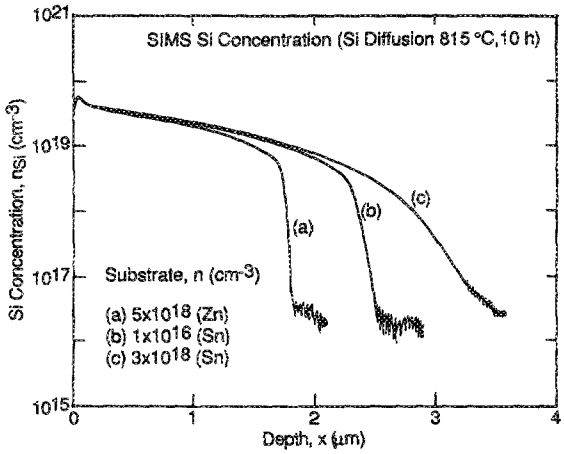

FIG. 17. SIMS profiles for Si diffusion at 815 °C (10 h) into GaAs of different background doping species and concentrations. The Si diffusion depth increases and the diffusion front becomes less steep as the background doping in the wafer changes from: (a) p-type, $n_{Zn} = 5\times10^{18}$ cm^{-3}; to (b) low doping $n_{Sn} = 10^{16}$ cm^{-3}; to (c) n-type, $n_{Sn} = 3\times10^{18}$ cm^{-3}. (From Ref. 66.)

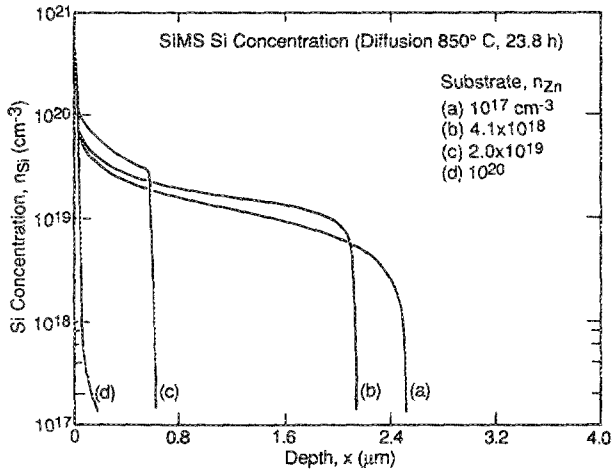

FIG. 16. SIMS profiles for 850 °C (23.8 h) Si diffusion into four GaAs wafers of Zn concentration, (a) $n_{Zn} = 10^{17}$, (b) 4.1×10^{18}, (c) 2×10^{19}, and (d) 10^{20} cm^{-3}. The Si diffusion depth decreases with n_{Zn}, and the concentration profiles n_{Si} become sharper. For $n_{Zn} = 10^{20}$ cm^{-3}, the Si diffusion is shallow and the crystal remains p-type. Type conversion occurs for (a), (b), and (c). (From Ref. 35.)

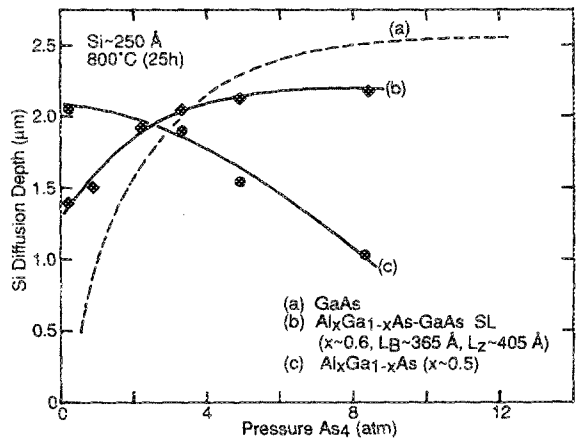

FIG. 18. Si diffusion depth vs As_4 overpressure data for Si-diffused samples: (a) bulk-crystal GaAs, (b) an Al_xGa_{1-x} As-GaAs superlattice (SL2, $x\sim0.6$, $L_B\approx365$ Å, $L_z\approx405$ Å), and (c) bulk-crystal $Al_xGa_{1-x}As$ ($x\sim0.5$). For both the bulk-crystal GaAs and SL2 the diffusion depth increases with increasing As_4 overpressure, but the opposite trend holds for $Al_xGa_{1-x}As$. (From Ref. 65.)

crystal, eventually saturates. Above this value the diffusion rate of the Si becomes relatively independent of the As vapor pressure.

Note that these arguments assume, however, that the role of the As vapor pressure in generating Column III vacancies is unaffected by the thin layer of elemental Si deposited on the crystal surface. As can be seen in Fig. 18, although similar results are found for the $Al_{0.6}Ga_{0.4}As$-GaAs SL, curve (b), quite different behavior is found when the Si is diffused into homogeneous $Al_{0.5}Ga_{0.5}As$, curve (c). The discrepancy most likely lies in the role of the Si layer deposited on the crystal surface. Kavanagh *et al.*[61] have studied a layer of elemental Si deposited on GaAs in which the Si layer contains either 0 or 12% As. In their study, they found that for elemental Si layers that contain no As, the Si-GaAs interface is chemically stable for anneals up to 1000 °C.[61] That is, no Si diffusion occurs into the GaAs crystal, and no outdiffusion of Ga or As occurs in the Si layer. When the Si layer is As-doped, however, not only does Si diffusion occur in the GaAs crystal, but also significant outdiffusion of Ga occurs into the Si film. Therefore, the Column III vacancies necessary for Si diffusion are not simply generated through the effect of the As vapor pressure, but also through the outdiffusion of Ga into the Si film, which is strongly controlled by the "chemistry" involving the Si, Ga, and excess As. This "chemistry" may be quite different for Si films deposited on $Al_xGa_{1-x}As$.

An important part of the Si diffusion is that it causes IILD of $Al_xGa_{1-x}As$-GaAs SLs.[5] The effects of As overpressure on the Si diffusion and subsequent layer intermixing in $Al_xGa_{1-x}As$-GaAs SLs has been studied by Ishida *et al.*[67] using SIMS and an ion implanted Si source. In this case, the As vapor pressure interacts only with the bare crystal surface. Ishida *et al.*[67] have found that the Si diffusion and IILD occur for the implanted source only when the crystal is annealed under a significant As overpressure, or with an SiO_2 cap which is known to generate Column III vacancies.[59,68,69] If no As overpressure or SiO_2 cap is applied on the experimental sample, the same anneal procedure results in not only no detectable Si diffusion, but also no IILD occurs in the SL even in the implanted regions.[67] These studies show the importance of the Column III vacancies in both the Si diffusion and the IILD which accompanies the diffusion.

Note that the discussion so far has focused only on the defects and diffusion that occur on the Column III sublattice. This is due, in part, to the lack of information on the Column V sublattice behavior from studies of just $Al_xGa_{1-x}As$-GaAs QWHs, and thus on only one type of Column V atom. However, Deppe *et al.*[70] have also studied the effect of Si diffusion on an $In_{0.5}Ga_{0.3}Al_{0.2}P$-GaAs heterointerface. Figure 19 shows a comparison, based on SIMS, of the quaternary-binary heterointerface for (a) thermal annealing at 850 °C (12 h) and for (b) Si diffusion at 850 °C (12 h). The thermal anneal at 850 °C (12 h), Fig. 19(a), causes little change in the atomic profiles of either the Column III or Column V lattice atoms. The Si diffusion, however, results in a large enhancement of the diffusion of the Column III lattice atoms In, Al, and Ga, while having little

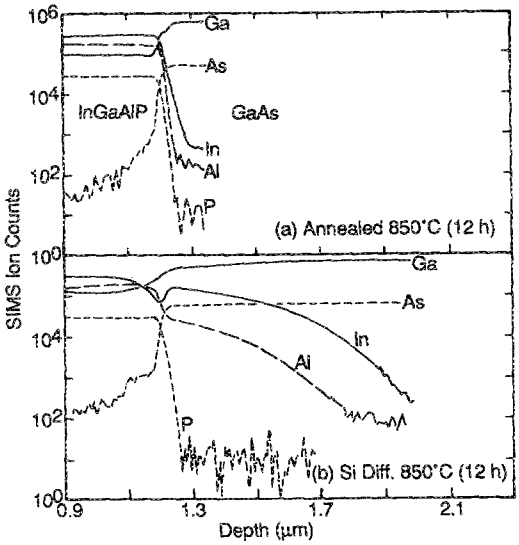

FIG. 19. SIMS profiles on an $In_{0.5}Al_{0.2}Ga_{0.3}P$-GaAs heterojunction after (a) annealing (12 h, 850 °C) and (b) Si diffusion (12 h, 850 °C). The heterojunction shows a large enhancement in self diffusion of the Column III lattice atoms (Al, In, and Ga), but little change in the Column V lattice atom (As and P) profiles due to the Si diffusion.

effect on Column V lattice atom diffusion. These data show that defects that accompany the Si diffusion are mainly associated with the Column III sublattice, consistent with the Column III vacancy diffusion on its own sublattice.

It has been assumed that the $Si_{III} - V_{III}$ complexes that are of concern here form due to the interaction between the positively charged Si_{III}^{+} (donorlike) and the Column III vacancy (acceptorlike). Based on this argument the Column III vacancy should complex with other donors as well. In fact, donor vacancy complexes in GaAs have been studied previously.[71-79] The binding energy of the complex is determined in part by the separation between the donor impurity and the Column III vacancy. Therefore, donor impurities such as S, Se, or Te that are located on Column V lattice sites and form nearest-neighbor complexes with the Column III vacancies are expected to have higher binding energies than the donors Si, Ge, or Sn. Hwang[72] has used photoluminescence to examine GaAs heavily doped with either Te or Si. By measuring the strength of the luminescence signal characteristic of donor vacancy complexes,[71-73] he has found (using thermal anneals) that the $Te_{As} - V_{Ga}$ complex is indeed more stable than the $Si_{Ga} - V_{Ga}$.[72]

Deppe *et al.*[66] have investigated the effects of background donor species, either the Column IV donor Sn or the Column VI donors Se or Te, on Si diffusion in GaAs. Figure 20 shows SIMS profiles of Si diffusion performed under identical conditions into GaAs containing either (a) Te, (b) Se, or (c) Sn. Although initial electron concentrations in all wafers are $3-4\times10^{18}$ cm^{-3}, shallower diffusions are found for the wafers doped with donors located on the Column V lattice. This trend can be understood by considering the increased binding energy of the Column VI donor Column III vacancy complex. For the Sn-doped wafer, due to the

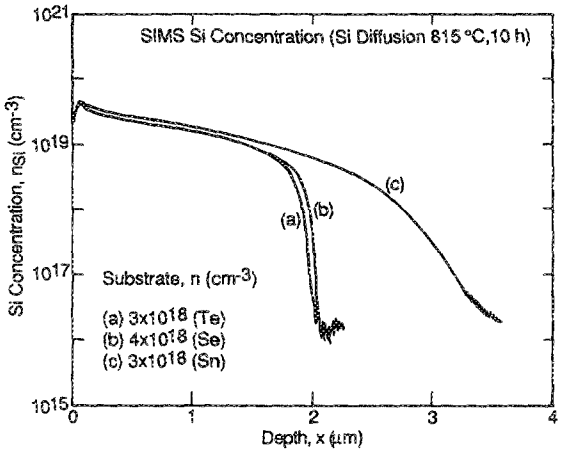

FIG. 20. SIMS profiles showing the different behavior of Si diffusion (815 °C, 10 h) in GaAs wafers containing the Column VI donors (a) $n_{Te} = 3\times10^{18}$ cm^{-3} or (b) $n_{Se} = 4\times10^{18}$ cm^{-3} compared to Column IV donor (c) $n_{Sn} = 3\times10^{18}$ cm^{-3}. (From Ref. 66.)

smaller binding energy of the $Sn_{Ga} - V_{Ga}$ complex, there will be more free Column III vacancies available to complex with the Si diffusant.

Using TEM, both Laister and Jenkins[78] and Hutchinson and Dobson[79] have found that dislocations form when wafers heavily doped with the donors Se or Te are subjected to high temperature anneals. As suggested by Hurle[74] the dislocations are due to a supersaturation of Ga interstitials and are formed through the reaction

$$Te_{As}^{+} \rightleftarrows (Te_{As} - V_{Ga})^{-} + I_{Ga} + 2h^{+}. \quad (31)$$

These various studies point to the importance of donor vacancy complexes in determining both donor diffusion behavior and IILD in $Al_xGa_{1-x}As$-GaAs crystals.

B. Zn diffusion

Perhaps the most studied diffusant in GaAs (and $Al_xGa_{1-x}As$) has been Zn, which is also the starting point for IILD.[1] Zinc diffusion in GaAs has been studied extensively. For recent reviews the reader is directed to those of Kendall[80] and Casey.[81] Here, we will review the diffusion of Zn in $Al_xGa_{1-x}As$ and GaAs in the light of its role in IILD[1] (see Fig. 1). After an early report by Allen and Cunnell,[82] more intense research began on the peculiar diffusion behavior of Zn in GaAs.[83–86] In 1961 Longini[86] proposed that Zn diffuses through an interstitial substitutional mechanism in which the Zn, as an interstitial, acts as a donor-type defect and diffuses rapidly. When located on a Column III lattice site, then, the Zn diffuses only slowly and is a shallow acceptor.[86] This model explains both the rapid diffusion rate of the Zn in GaAs and also the Zn concentration dependence found for the diffusion rate. Since the substitutional Zn has a high solubility as an acceptor impurity, the large hole concentration due to the Zn diffusion increases the solubility of the rapidly diffusing donorlike interstitial Zn.[31,32,86] Shih *et al.*[87,88] have measured the dependence of the Zn diffusion on As vapor pressure and have found consistency with the Longini[86] diffusion model. As the As vapor pressure increases, more Column III sites become available for the Zn to occupy substitutional sites, and the Zn diffusion rate becomes slower.[88]

In early work, it was assumed that Column III sites become available for the interstitial Zn by the diffusion of Column III vacancies from either the crystal surface or dislocations in the crystal bulk. In 1970, however, Winteler[89] proposed that Column III sites become available through a Frenkel reaction on the Column III sublattice, i.e., Eq. (2). In this case, the rate at which the GaAs crystal can create Column III vacancies will be partly determined by Column III interstitial diffusion rates as opposed to those of Column III vacancies.[89] In 1981, Gösele and Morehead[90] suggested that the Column III interstitial is created directly by an interstitial Zn moving into a Column III lattice site through a "kick-out" mechanism, i.e.,

$$Zn_I^{+} + \rightleftarrows Zn_{III}^{-} + I_{III}^{+} + 2h^{+}. \quad (32)$$

Since the substitutional Zn_{III}^{-} concentration due to Zn diffusion in GaAs is typically $\gtrsim 5\times10^{19}$ cm^{-3}, reaction (32) suggests that the Zn-diffused regions will contain a high concentration of Column III interstitial defects. Consistent with earlier discussions on layer intermixing in undoped and *p*-type QWHs,[13,37–39] this high concentration of Column III interstitial defects offers a basis for IILD [see Eq. (5)] via Zn diffusion that was first discovered by Laidig *et al.*[1] as discussed above. Although the Column III interstitial defects are expected to have rapid diffusion rates, as can be seen from Fig. 1, the IILD in $Al_xGa_{1-x}As$-GaAs SLs is localized to the Zn-diffused regions. This is due to the increased solubility of the donor-type Column III interstitial defects[31,32] in the heavily *p*-type Zn-diffused region.

Since the initial discovery of IILD via Zn diffusion,[1] there have been many other studies of Zn diffusion in III-V QWHs.[55,91–101] Both Nakashima *et al.*[100] and Deppe *et al.*[101] have used SIMS to analyze the effect of low-temperature Zn diffusion on Column V lattice atom diffusion. Nakashima *et al.*[100] have investigated Zn diffusion in an InP-$In_{0.53}Ga_{0.47}As$ SL, while Deppe *et al.*[101] have investigated in higher energy-gap material the Zn diffusion behavior at an $In_{0.5}Ga_{0.2}Al_{0.3}P$-GaAs heterointerface. Figure 21 shows the SIMS profile of the $In_{0.5}Ga_{0.2}Al_{0.3}P$-GaAs heterointerface for (a) the "as-grown" crystal and (b) after Zn diffusion at 600 °C for 20 h. While the profiles of the lattice atoms are relatively sharp in the "as-grown" crystal, Fig. 21(a), after the Zn diffusion the Column III lattice atoms In and Al show significant diffusion into the GaAs crystal. A significant change also occurs in the Ga profile, although it is not as obvious in Fig. 21 since Ga exists on both sides of the heterojunction in the as-grown crystal. It is important to note, however, that the diffusing Zn impurity does not enhance diffusion of the Column V lattice atoms, i.e., the As or P. The As and P SIMS profiles of the Zn-diffused heterojunction, Fig. 21(b), remain nearly identical to those of the as-grown crystal, Fig. 21(a). Similar results have been obtained by Nakashima *et al.*[100] The enhancement of diffusion of only the Column III lattice atoms is consistent with the Column III interstitial mechanism discussed above, which involves defects only on the Column III lattice.

Camras *et al.*[93] have shown that layer intermixing due to

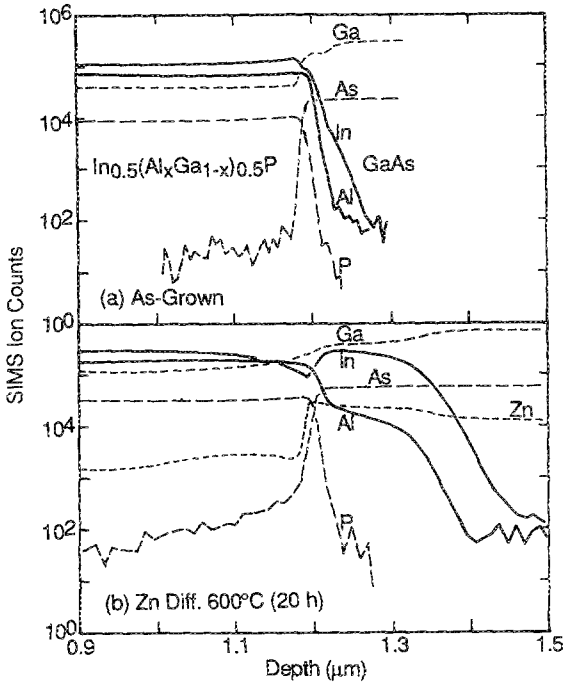

FIG. 21. SIMS profiles at an $In_{0.5}(Al_{0.4}Ga_{0.6})_{0.5}P$-GaAs heterointerface (1.2 μm depth) for (a) the "as-grown" crystal and (b) after Zn diffusion (600 °C, 20 h). The Column III atoms In, Al, and Ga of the crystal show an enhanced self-diffusion rate; however, little change occurs in the profiles of the Column V atoms As and P. (From Ref. 101.)

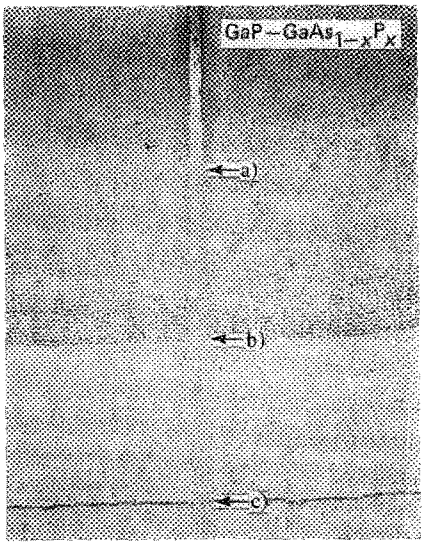

FIG. 22. Shallow angle cross section of a SL (grown by MOCVD) consisting of 40 periods of $L_z \sim 120$ Å $GaAs_{1-x}P_x$ ($x \sim 0.6$) quantum wells coupled by $L_B \sim 120$ Å GaP barriers. Zn is diffused (825 °C, 14 h) through a 24-μm mask opening and intermixes the layers [regions (a)–(b)] but not the region under the Si_3N_4 mask. (Note that the shallow angle cross sectioning results only in vertical but not horizontal "magnification.") (From Ref. 93.)

Zn diffusion can also occur for a GaP-$GaAs_xP_{1-x}$ SL as shown in Fig. 22. An understanding of the intermixing is complicated, however, by the large amount of strain in the as-grown crystal. Also, the Zn-diffusion temperature used in this study[93] was 825 °C, much higher than typically used for IILD via Zn diffusion. Column V vacancies are expected to act as donor-type defects, and thus will have an increased solubility due to the heavy p-type Zn doping.[32,34] At the higher anneal temperature of 825 °C, Column V vacancies may have a significant diffusion rate, leading to the layer intermixing found in the Zn-diffused GaP-$GaAs_{1-x}P_x$ SL.[93]

Note that complex formation, much as discussed earlier in the case of Si diffusion, may also be important for Column III acceptor diffusion. Recently Houston *et al.*[102] have shown that Zn diffusion into $Al_xGa_{1-x}As$ or GaAs containing Be-doped regions causes extremely rapid diffusion of the grown-in Be. They have suggested that swapping between diffusing interstitial Zn and substitutional Be, i.e.,[102]

$$Zn_I^{+\,+} + Be_s^{-} \rightleftarrows Zn_s^{--} + Be_I^{+\,+}, \tag{33}$$

occurs because of the Zn having an atomic radius which more closely matches that of the Ga. The interstitial Be can then diffuse very rapidly, causing the Be redistribution. It may be a natural consequence, however, for all acceptor impurities to undergo the swapping between interstitial and substitutional sites as expressed by reaction (33). That is, the reaction

$$Zn_I^{+\,+} + Zn_s^{-} \rightarrow Zn_s^{--} + Zn_I^{+\,+} \tag{34}$$

may also be heavily favored for diffusing Zn since the Coulomb attraction will tend to complex the positively charged interstitial $Zn_I^{+\,+}$ with the negatively charged substitutional Zn_{III}^{--}. Since, in the presence of diffusing Zn (or Be, or Mg, for example) we expect a large concentration of Column III interstitial defects, we can also expect to some degree the reverse of reaction (32) to occur, i.e.,

$$I_{III}^{+\,+\,+} + Zn_{III}^{--} \rightarrow Zn_I^{+\,+} + 2e^{-}. \tag{35}$$

At low acceptor concentrations (at the Zn diffusion front, for instance) we expect reaction (35) to proceed to the left simply because the concentration of Column III lattice atoms will be much greater than that of the substitutional acceptor impurity.

IV. IMPURITY-INDUCED LAYER DISORDERING VIA ION IMPLANTATION

Ion implantation of many different atomic species has been shown to promote intermixing of $Al_xGa_{1-x}As$-GaAs QWHs and SLs.[6,7,8,15-18,67,103-125] Initial experiments have shown that the commonly used shallow impurities Si[6,7] and Zn[8] are effective in IILD from ion implanted sources. Gavrilovic *et al.*[15] have shown also that implantation damage can promote IILD upon a subsequent anneal. Figure 23 shows a shallow angle cross section of an AlAs-GaAs SL implanted with Kr and then annealed at 850 °C for 8 h.[15] As can be seen in the cross section, complete layer intermixing occurs in the implanted region, while the unimplanted region of the SL remains stable. Ralston *et al.*[16] have shown that the layer intermixing due to lattice damage is correlated to the mass of the implanted species. In contrast, shallow acceptor and donor species are expected to promote layer intermixing, in a

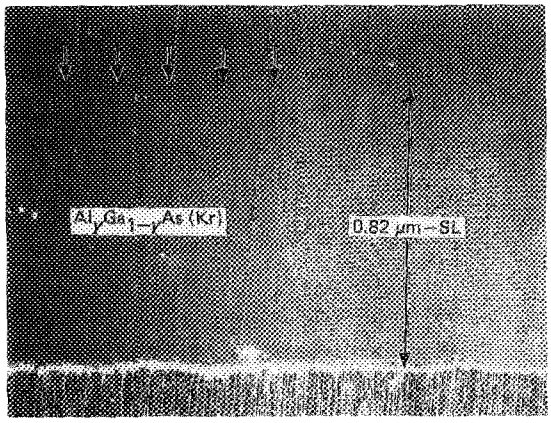

FIG. 23. Slant cross section of an AlAs-GaAs SL crystal implanted with Kr^+ ($10^{15}/cm^2$, 390 keV) and annealed at 850 °C for 8.33 h. The SL has been masked with 0.5 mm dots on 1 mm centers. The Kr implantation (and annealing, left-hand side) results in complete disordering. (From Ref. 15.)

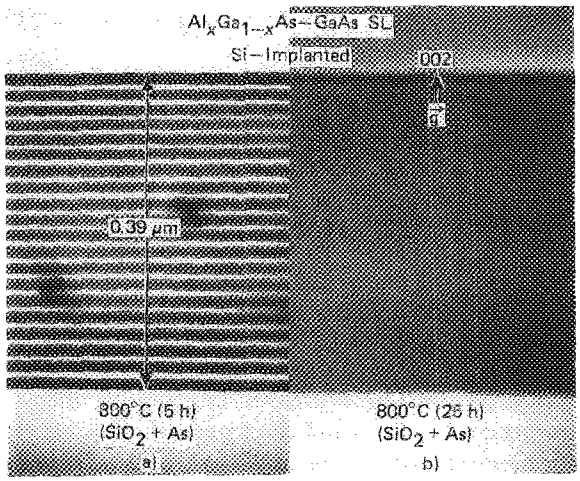

FIG. 25. TEM cross sections of the Si-implanted SL of Fig. 24 (400 keV, $5\times10^{13}/cm^2$) showing the evolution of Si^+-IILD on annealing with the samples capped with SiO_2. Complete Si^+-IILD is achieved after 25 h annealing. (From Ref. 110.)

large part, through the doping and diffusion mechanisms described in Secs. II and III. The Si impurity, in particular, has received a great deal of attention as a disordering agent of $Al_xGa_{1-x}As$-GaAs SLs when introduced via ion implantation.[6,7,18,67,103-117] For the most part, its role in SL layer intermixing when implanted is consistent with its behavior when diffused into the crystal from an external source. Guido *et al.*[110] have shown that a Si-implanted $Al_xGa_{1-x}As$-GaAs SL must be annealed under conditions that promote the Si diffusion, that is, create Column III vacancies, for IILD to occur. They have used TEM cross sections to study the layer intermixing of a Si-implanted (400 keV, 5×10^{13} cm^{-2}) $Al_xGa_{1-x}As$-GaAs SL for sample anneals at 800 °C of either 5 or 25 h. Figure 24 shows a TEM cross section of the SL when annealed with a Si_3N_4 cap.[110] The Si_3N_4 layer is known to block the out-diffusion of Ga, thus inhibiting Column III vacancy generation.[68] Under this annealing condition, only slight layer intermixing occurs. However, when the Si-implanted SL is annealed under conditions favoring Column III vacancy generation, such as with an SiO_2 cap,[68,69] Fig. 25, or capless with a large As overpressure, Fig. 26, complete layer intermixing occurs for an 800 °C, 25 h anneal. Ishida *et al.*[67] have shown more directly using SIMS that for a Si-implanted $Al_xGa_{1-x}As$-GaAs SL layer intermixing occurs only when Si diffusion occurs. Compensation of the implanted Si by coimplanting Be has been found by Kobayashi *et al.*[109] to suppress IILD, similar to results found for grown-in impurities.[51] Although IILD due to Si implantation is similar in many ways to that of simple Si diffusion from an external source, there also exist some interesting differences. Layer intermixing in $Al_xGa_{1-x}As$-GaAs SLs is inhibited in regions near the Si implant peak when a heavy implant dose is used.[104,106] Although the reason for this is not fully under-

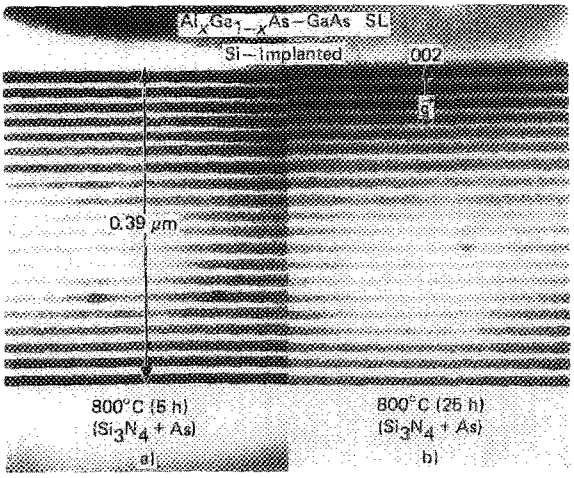

FIG. 24. TEM cross sections of a Si-implanted SL (400 keV, $5\times10^{13}/cm^2$) showing the evolution of Si^+-IILD with annealing (800 °C, 5 → 25 h, samples capped with Si_3N_4). Layer disordering is observed to saturate as the annealing time is increased. (From Ref. 110.)

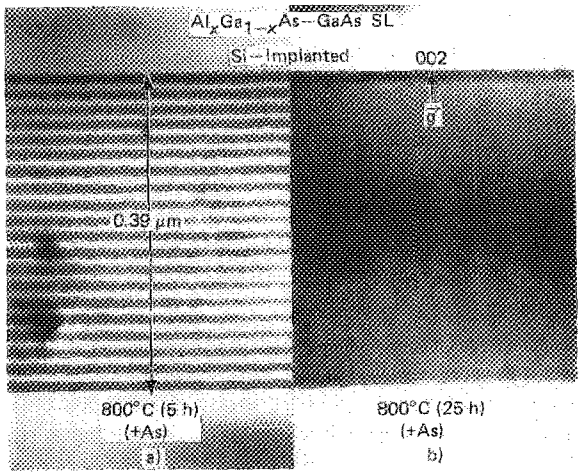

FIG. 26. TEM cross section of the Si-implanted SL of Figs. 24 and 25 (400 keV, $5\times10^{13}cm^2$) showing the evolution of Si^+-IILD with capless annealing. Complete Si^+-IILD is achieved after 25 h annealing. (From Ref. 110.)

stood, it seems to be related to unusually large defect concentrations.[104,106,111]

As mentioned earlier, under certain conditions lattice damage due to ion implantation can be used to cause QWH layer intermixing.[15–18,118–123] This offers the advantage of selectively intermixing regions of a QWH without significantly altering the crystal conductivity if ions such as Al,[15,123] Ga,[17,119–122] or As[18,118] (lattice constituents) are used. Although detailed mechanisms for the layer intermixing due to lattice damage are not yet understood, it is clear that an increase of point defects such as Column III vacancies or Column III interstitials will lead to increased lattice atom diffusion, i.e., Eq. (6). Moreover, implanting either Al or Ga can presumably favor diffusion through the Column III interstitial mechanism in the implanted regions (regions rich with Column III lattice atoms).

Mei *et al.*[124] have performed comparative studies for implanted SLs in which the ion implantation species are of similar mass but different electronic valence, i.e., Ga, Ge, and As or of different mass but similar valence, i.e., Ge and Si. For these implanted species they have found that, as expected, the valence of the implanted ion is most important in determining the amount of intermixing.[124] The mass of the implanted species is a second-order effect important when no change in the free carrier concentration occurs.

V. DEVICE APPLICATIONS

Beyond its intrinsic interest, impurity-induced layer disordering is an important process for III-V device fabrication, because it readily allows the fabrication of heterojunctions perpendicular to the thin epitaxial layers characteristic of QWHs.[4] This process can then be used to fabricate devices with three-dimensional carrier and photon confinement using standard masking procedures of the crystal surfaces and either selective impurity diffusion or ion implantation. These properties make the IILD well suited to the fabrication of both buried heterostructure QW laser diodes and to optical waveguides, which are also expected to be integral elements in optoelectronic integrated circuits. It is likely that the IILD will find application in other types of devices as well. Early work on the IILD in $Al_xGa_{1-x}As$-GaAs via Zn diffusion focused on characterizing the "disordered" crystal and in patterning the layer disordering.[4,95] Also, the thermal stability of laser device structures either with no doping or with only the *p* and *n* doping necessary for current injection into the laser active region has also been investigated.[21,126,127] This information is important in order to determine the limits at which thermal processing of the devices begins to degrade performance, i.e., interferes with IILD and its selective operation.

Meehan *et al.*[128] have described the first semiconductor laser diodes utilizing IILD via Zn diffusion. However, the device structure suffered from large shunt leakage currents around the diode active region because of large area parasitic *p-n* junctions formed by the Zn diffusion. In accord with the patent of Ref. 4, this parasitic *p-n* junction area can be reduced. This has been demonstrated by Fukuzawa *et al.*[129] by performing the Zn diffusion, and accompanying layer disordering outside of the stripe geometry laser active region, on *p*-substrate QWHs grown with *n*-type upper confining layers. Meehan *et al.*[5] next demonstrated that the *n*-type impurity Si could be used for IILD in an $Al_xGa_{1-x}As$-GaAs SL when diffused from an external source, and used the process to fabricate buried heterostructure QW laser diodes grown in the more standard form of *p*-type upper layers on *n*-type lower layers, with an *n*-type substrate underneath.[130] Since these early developments, there has been much research effort directed toward using IILD for the fabrication of semiconductor laser diodes,[131–162] optical waveguides,[163–166] and also an optical detector.[167] Buried heterostructure laser diodes and waveguide structures have also been fabricated using IILD via ion implantation[139,147] and most recently laser assisted incorporation of impurities into the crystal.[156,159]

Figure 27 shows a scanning electron microscope (SEM) image of the cross section of an IILD (via Si diffusion) buried heterostructure QW laser diode.[140] The active region of the device consists of two 70 Å GaAs QWs separated by a 110 Å $Al_{0.35}Ga_{0.65}As$ barrier, with barrier and wells sandwiched in a 0.2 μm $Al_{0.35}Ga_{0.65}As$ waveguide region. A Se-doped *n*-type $Al_{0.85}Ga_{0.15}As$ lower confining layer and a Mg-doped *p*-type $Al_{0.85}Ga_{0.15}As$ upper confining layer complete the structure. A 0.1 μm heavily Zn-doped p^+ contact layer is grown on the upper *p*-type $Al_{0.85}Ga_{0.15}As$ confining layer in order to aid low resistance metal contact to the device. The Si diffusion, which has been masked by a 5 μm Si_3N_4 stripe, can be seen in Fig. 27 to extend on either side of the active region into the lower *n*-type $Al_{0.85}Ga_{0.15}As$ confining layer. The Si diffusion converts the crystal to *n* type and thus forms a current constraining *p-n* junction in the high gap upper Mg-doped $Al_{0.85}Ga_{0.15}As$ confining layer. Most important, as the Si diffuses through the QW active region, layer intermixing occurs between the GaAs QWs and the $Al_{0.35}Ga_{0.65}As$ waveguide, and also between the waveguide region and the upper and lower $Al_{0.85}Ga_{0.15}As$ confining layers. The layer intermixing results in an increased band gap, relative to the masked undiffused active region preserved beneath the Si_3N_4 mask, thus giving a built-in lateral refractive index step that provides optical confinement. The *p-n* junction formed in the upper confining layer because of

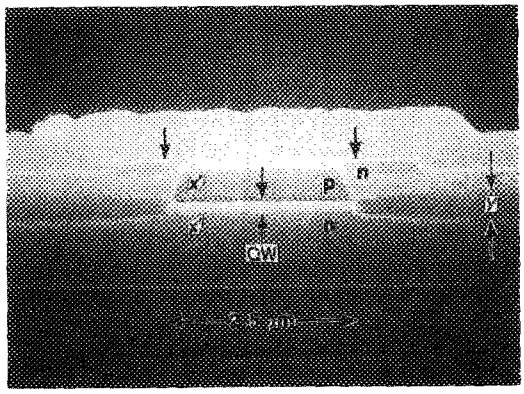

FIG. 27. Scanning electron microscope image of a QWH stripe geometry laser with Si diffusion (850 °C, 9.5 h) and layer disordering (intermixing) on the right and left-hand sides. Lateral diffusion of the Si has narrowed the active region to ~2.5 μm. (From Ref. 140.)

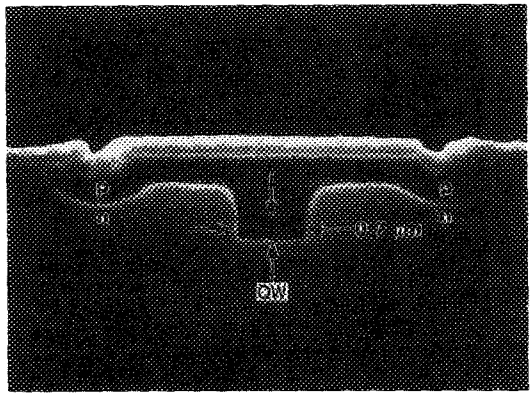

FIG. 28. Scanning electron microscope image of the stripe region of an IILD stripe geometry QWH laser after metallizaton. The metallization causes the p region to etch much more heavily than in Fig. 27. This sample has been Si diffused on the left and right-hand for 20 h at 850 °C. Lateral Si diffusion shrinks the active region width to 0.7 μm (marked by horizontal arrows). (From Ref. 140.)

the Si diffusion provides current confinement in the laser active region since the high gap junction and the diode active region have different "turn on" voltages. This form of IILD buried heterostructure offers the advantage of a simplified fabrication process over that of, say, regrown laser diode structures. By utilizing the lateral diffusion of the Si under the Si_3N_4, we find it possible to obtain narrower active region widths than shown in Fig. 27 and thus lower lasing thresholds. Increasing the diffusion time from 9.5 to 20 h results in a narrower laser active region ($2.5 \rightarrow 0.7$ μm).[140]

Figure 28 shows an SEM cross section of the metallized laser diode structure with the 0.7 μm active region. A shallow Zn diffusion has been performed on the structure after the Si diffusion to move all p-n junctions, except at the laser active region, into the high gap $Al_{0.85}Ga_{0.15}As$ upper confining layer. The narrow active region width results in a low continuous wave (cw) laser threshold of 3 mA as shown in Fig. 29.[140] Similar low threshold laser diode performance has also been obtained by Thornton *et al.*[141] using IILD via Si diffusion.

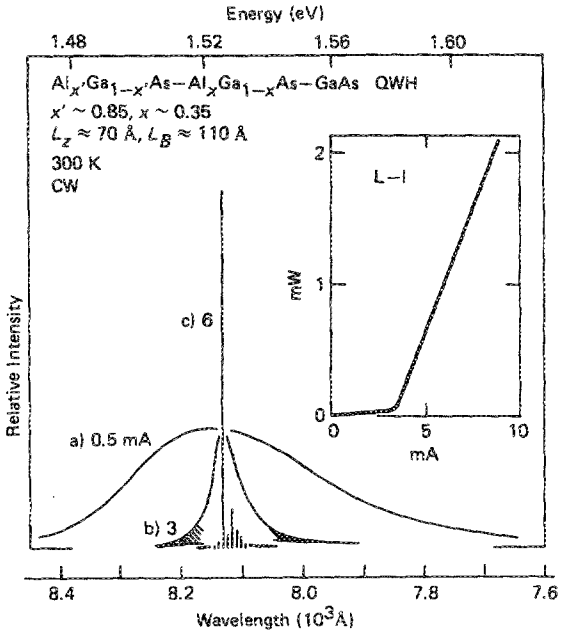

FIG. 29. Room-temperature cw output spectra and L-I curve (inset) for the IILD stripe-geometry $Al_xGa_{1-x}As$-GaAs QWH laser diode of Fig. 28 with 0.7-μm-wide active region and 250-μm-long cavity. The laser operation is single mode at 4.5 mA and remains single mode through the entire operating range. (From Ref. 140.)

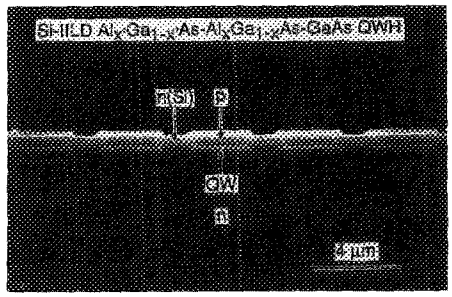

FIG. 30. Cross section (via scanning electron microscope) of a ten stripe Si IILD $Al_xGa_{1-x}As$-GaAs laser array. The QWH emitter widths are 3 μm wide with a 1-μm disordered region separating them. The Si diffusion is performed at 816 °C (10 h). (From Ref. 152.)

Impurity-induced layer disordering of p-n $Al_xGa_{1-x}As$-GaAs QWHs also provides a convenient means to fabricate index guided multiple stripe laser diodes capable of high cw output powers. The first multiple stripe laser diodes fabricated did not operate optically coupled because of the strong index guiding of the IILD regions.[135,142] However, by reducing the IILD region width to a 1 μm separation between adjacent laser stripes, and a center-to-center stripe spacing of 4 μm, optical coupling of an IILD multiple stripe laser has been achieved.[152] Figure 30 shows an SEM cross section of the 10 stripe laser, and Fig. 31 shows the corresponding cw L-I curve and spectrum. The predominantly twin lobed far field radiation pattern of the 10 stripe

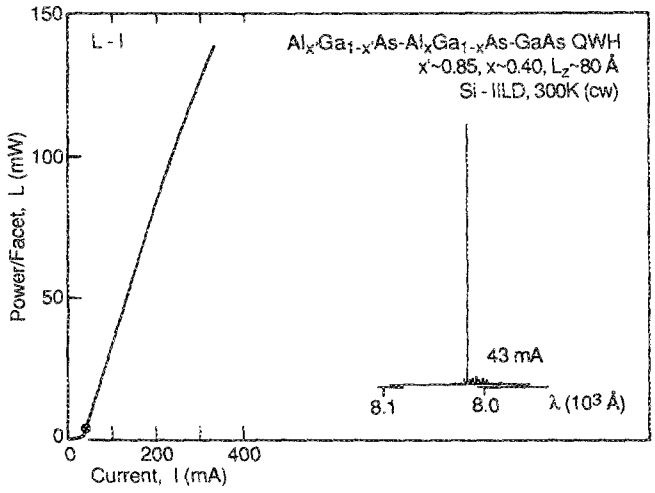

FIG. 31. Continuous (cw) 300 K light power vs current (L-I) and lasing spectrum just above threshold for the coupled-stripe $Al_xGa_{1-x}As$-GaAs laser array of Fig. 30. The differential efficiency at 200 mA (both laser facets) is 67%. At 325 mA the overall efficiency is 54%. (From Ref. 152.)

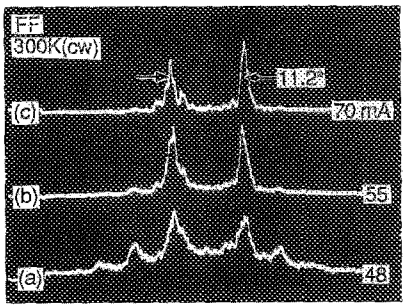

FIG. 32. Far field (FF) emission pattern of the ten stripe Si-IILD $Al_xGa_{1-x}As$-GaAs QWH laser array of Fig. 30. The FF pattern indicates operation in the highest order coupled mode of the ten stripe array. At (a) 48 mA, four peaks are resolved, with the inner pair also observed at (b) 55 mA and at (c) 70 mA and a spacing of 11°, or nearly the predicted value of 11.5° for a 4-μm NF pattern. The two outer peaks (21.7° apart) are due to higher order interference effects. At (c) 70 mA the two peaks have a FWHM of 1.37°, which indicates single supermode operation. (From Ref. 152.)

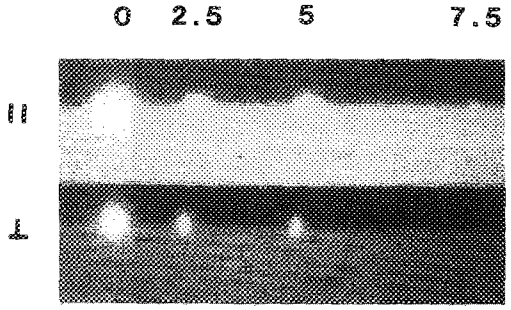

FIG. 33. Infrared television images of the transmitted mode patterns through waveguides formed by IILD on an $Al_xGa_{1-x}As$-GaAs QWH. At waveguide bend angles ranging from 0, 2.5, 5, to 7.5° the near field images (at a cleaved facet) decrease, showing bends to $\sim$ 7° are possible. (From Ref. 164.)

laser, shown in Fig. 32, suggests that adjacent stripes operate in an out of phase optical mode.

So-called window lasers, in which the effective active region energy gap has been increased at the laser facets as shown in Ref. 4, have also been fabricated using IILD. Suzuki *et al.*[131] have shown that IILD window lasers made using Zn diffusion exhibit an increase from 40 to 120 mW optical power output under pulsed operation before laser facet damage occurs. However, the Zn diffusion results in a very high free-carrier concentration ($\gtrsim 5\times10^{19}$ cm^{-3}) in the diffused regions and both the laser threshold and efficiency suffer due to free-carrier absorption.[131,138] Thornton *et al.*[150] have utilized Si diffusion for IILD and obtained much better results from window lasers. For a multiple stripe QWH laser structure maximum optical power out has been increased by a factor of 4 for lasers with disordered windows, an increase from 0.5 W to over 2 W cw.[150]

From the extensive work on buried heterostructure laser diodes and the active waveguide regions incorporated in various laser structures, it is apparent that IILD is an effective way to fabricate also passive optical waveguides, which are expected to be important components in optoelectronic integrated circuits. Some research on optical waveguides fabricated in III-V QWHs has been reported.[163-166] For use in optoelectronic integrated circuits one important parameter will be, of course, the maximum angle at which the waveguide can bend the light and maintain some level of confinement and transmission in the waveguide. Although this maximum angle will most likely depend strongly on the QWH design and the IILD process used, some initial results have been reported by Julien *et al.*[164] for waveguides fabricated using Zn diffusion. Figure 33 shows transmitted mode patterns of light ($\lambda\sim871$ mm) for waveguides with abrupt bends of varying angles. For the parallel polarized optical mode some light is transmitted through the waveguide even at angles of $\sim$7.5°. For the perpendicular polarized mode transmission cuts off at $\sim$ 5°. Swanson *et al.*[165] have increased the bend angle at which the waveguide transmission has a 3 dB loss from 3° for an abrupt bend to 7° by varying the waveguide geometry.

VI. SUMMARY

In this review, we have considered in some detail the process of impurity-induced layer disordering in III-V QWHs, mainly in $Al_xGa_{1-x}As$-GaAs because of the success of IILD in this system. The layered structures and heterostructures offer the unique opportunity to track easily crystal properties such as self-diffusion, as well as the role of impurity diffusion in crystal self-diffusion. This, in turn, offers important clues concerning the defect mechanisms through which diffusion processes take place. As opposed to elemental semiconductors, the sensitivity of the defect concentrations in compound semiconductors to the surface conditions during annealing has provided considerable insight into which defects may be most important in diffusion processes and in layer disordering (intermixing).

The $Al_xGa_{1-x}As$-GaAs crystal system is unique in respect to the close lattice match between AlAs and GaAs. This "built-in" lattice match is particularly fortuitous for the utilization of IILD. Studies of diffusion processes, especially self-diffusion processes, are at a much more primitive stage in some of the other important III-V semiconductors such as the InP-$In_xGa_{1-x}As_yP_{1-y}$ heterosystem. The constraint of close lattice matching for reliable device operation may make the application of IILD to this important lower gap quaternary system less attractive. We mention, however, that any thin layer heterosystem, specifically QWHs or SLs, is a candidate for some form of layer intermixing simply because of the advantageous thin layer geometry and the ease or advantage in intermixing thin layers. In other words, various schemes might exist or be found to intermix and to "average" thin layers or "to absorb" a quantum well layer in thicker barrier layers.

In any case, IILD has been found to be a very useful process for device fabrication in the $Al_xGa_{1-x}As$-GaAs QWH system. The capability to fabricate high performance buried heterostructure lasers and passive waveguides employing impurity diffusion or ion implantation, an integrated circuit (IC) type of processing, may ultimately prove highly desirable for optoelectronic integrated circuits. Also, IILD is one of the few present day processes that has the potential to allow the fabrication of quantum well wires or

quantum well boxes, structures with novel device implications in spite of the fact that now QW wires or boxes are in a very primitive state, not to mention not available in dense arrays. For example, if the QWH (SL) dots of Fig. 2 (formed by IILD) can be made small enough in diameter and be made dense enough, and be incorporated into the active region of a *p-n* QWH diode, then the result will be an ultimate form of current driven laser. To realize these advances will require a more detailed knowledge of the mechanisms and characteristics of IILD and, of course, will require also further development of more sophisticated methods of pattern definition, masking procedures, and crystal processing.

ACKNOWLEDGMENTS

We are indebted to a number of colleagues for their interest and help in IILD studies. We wish to mention R. D. Burnham (Amoco), M. D. Camras (Hewlett–Packard), M. G. Craford (Hewlett-Packard), J. E. Epler (Xerox), P. Gavrilovic (Polaroid), L. J. Guido (Urbana), R. W. Kaliski (Ford), K. Meehan (Polaroid), and D. W. Nam (Urbana). We are grateful to many colleagues and various others for the use of their published figures. This work has been supported by Army Research Office Contract No. DAAG-29-85-K-0133, National Science Foundation Grants Nos. DMR-86-12860 and CDR-85-22666, and the Physical Electronics Associates Program.

[1]W. D. Laidig, N. Holonyak, Jr., M. D. Camras, K. Hess, J. J. Coleman, P. D. Dapkus, and J. Bardeen, Appl. Phys. Lett. **38**, 776 (1981).
[2]Since QWHs and SLs tend to confine phonons as well as electrons and holes, the purpose of these experiments, suggested by one of us (N.H.), was to search, in an initially undoped SL that required further doping, for phonon replicas involving an impurity (Zn) in radiative recombination. Hence, the Zn diffusion and the discovery of layer intermixing or disordering.
[3]L. L. Chang and A. Koma, Appl. Phys. Lett. **29**, 138 (1976).
[4]N. Holonyak, Jr., W. D. Laidig, M. D. Camras, J. J. Coleman, and P. D. Dapkus, Appl. Phys. Lett. **39**, 102 (1981). See also, N. Holonyak, Jr. and W. D. Laidig, U. S. Patent 4,378,255, March 29, 1983 (Filed May 6, 1981).
[5]K. Meehan, N. Holonyak, Jr., J. M. Brown, M. A. Nixon, P. Gavrilovic, and R. D. Burnham, Appl. Phys. Lett. **45**, 549 (1984).
[6]The first impurity implantation of $Al_xGa_{1-x}As$-GaAs SLs for layer disordering was performed for N. Holonyak, Jr. in early 1981 by M. Feng (then at Hughes Research) based on a request to Feng by G. E. Stillman. See N. Holonyak, Jr., U. S. Patent 4,511,408, April 16, 1985 (Filed April 22, 1982).
[7]J. J. Coleman, P. D. Dapkus, C. G. Kirkpatrick, M. D. Camras, and N. Holonyak, Jr., Appl. Phys. Lett. **40**, 904 (1982).
[8]M. D. Camras, J. J. Coleman, N. Holonyak, Jr., K. Hess, P. D. Dapkus, and C. G. Kirkpatrick, *Proceedings of the 10th International Symposium on GaAs and Related Compounds, Albuquerque,* 1982, edited by G. E. Stillman (Institute of Physics, London, 1983), pp. 233–239.
[9]M. Kawabe, N. Matsuura, N. Shimizu, F. Hasegawa, and Y. Nannichi, Jpn. J. Appl. Phys. **23**, L623 (1984).
[10]R. W. Kaliski, P. Gavrilovic, K. Meehan, J. Gavrilovic, K. C. Hsieh, G. S. Jackson, N. Holonyak, Jr., J. J. Coleman, R. D. Burnham, R. L. Thornton, and T. L. Paoli, J. Appl. Phys. **58**, 101 (1985).
[11]E. V. K. Rao, H. Thibierge, F. Brillouet, F. Alexandre, and R. Azoulay, Appl. Phys. Lett. **46**, 867 (1985).
[12]E. V. K. Rao, P. Ossart, F. Alexandre, and H. Thibierge, Appl. Phys. Lett. **50**, 588 (1987).
[13]R. W. Kaliski, D. W. Nam, D. G. Deppe, N. Holonyak, Jr., K. C. Hsieh, and R. D. Burnham, J. Appl. Phys. **62**, 998 (1987).
[14]N. Kamata, K. Kobayashi, K. Endo, T. Suzuki, and A. Misu, Jpn. J. Appl. Phys. **26**, 1092 (1987).
[15]P. Gavrilovic, D. G. Deppe, K. Meehan, N. Holonyak, Jr., J. J. Coleman, and R. D. Burnham, Appl. Phys. Lett. **47**, 130 (1985).
[16]J. Ralston, G. W. Wicks, L. F. Eastman, B. C. DeCooman, and C. B. Carter, J. Appl. Phys. **59**, 120 (1986).
[17]Y. Hirayama, Y. Suzuki, S. Tarucha, and H. Okamoto, Jpn. J. Appl. Phys. **24**, L516 (1985).
[18]Y. Hirayama, Y. Suzuki, and H. Okamoto, Jpn. J. Appl. Phys. **24**, 1498 (1985).
[19]J. E. Epler, R. D. Burnham, R. L. Thornton, T. L. Paoli, and M. C. Bashaw, Appl. Phys. Lett. **49**, 1447 (1986).
[20]R. M. Fleming, D. B. McWhan, A. C. Gossard, W. Wiegmann, and R. A. Logan, J. Appl. Phys. **51**, 357 (1980).
[21]M. D. Camras, N. Holonyak, Jr., R. D. Burnham, W. Streifer, D. R. Scifres, T. L. Paoli, and C. Lindström, J. Appl. Phys. **54**, 5637 (1983).
[22]T. E. Schlesinger and T. Kuech, Appl. Phys. Lett. **49**, 519 (1986).
[23]P. M. Petroff, J. Vac. Sci. Technol. **14**, 973 (1977).
[24]B. Goldstein, Phys. Rev. **121**, 1305 (1961).
[25]D. L. Kendall, in *Semiconductors and Semimetals,* edited by R. K. Willardson and A. C. Beer (Academic, New York, 1968), Vol. 4, Chap. 3, pp. 163–259.
[26]H. D. Palfrey, M. Brown, and A. F. W. Willoughby, J. Electrochem. Soc. **128**, 2224 (1981).
[27]H. D. Palfrey, M. Brown, and A. F. W. Willoughby, J. Electron. Mater. **12**, 863 (1983).
[28]A. F. W. Willoughby, in *Defects in Semiconductors II,* Vol. 14, Mater. Res. Soc. Symp. Proc., edited by S. Mahajan and J. W. Corbett (Elsevier, New York, 1983), pp. 237–252.
[29]J. R. Manning, *Diffusion Kinetics for Atoms in Crystals* (Van Nostrand, Princeton, 1968), pp. 95, 166.
[30]C. Wagner and K. Grunewald, Z. Phys. Chem. B **40**, 455 (1938).
[31]H. Reiss, J. Chem. Phys. **21**, 1209 (1953).
[32]R. L. Longini and R. F. Greene, Phys. Rev. **102**, 992 (1956).
[33]W. Shockley and J. L. Moll, Phys. Rev. **119**, 1480 (1960).
[34]T. Y. Tan and U. Gösele, J. Appl. Phys. **61**, 1841 (1987).
[35]D. G. Deppe, N. Holonyak, Jr., F. A. Kish, and J. E. Baker, Appl. Phys. Lett. **50**, 998 (1987).
[36]R. L. S. Devine, C. T. Foxon, B. A. Joyce, J. B. Clegg, and J. P. Govers, Appl. Phys. A **44**, 195 (1987).
[37]D. G. Deppe, L. J. Guido, and N. Holonyak, Jr., Materials Research Society, Spring Meeting, April 5–9, 1988, Reno, Mater. Res. Soc. Symp. Proc. **126**, 31 (1988).
[38]D. G. Deppe, N. Holonyak, Jr., W. E. Plano, V. M. Robbins, J. M. Dallesasse, K. C. Hsieh, and J. E. Baker, J. Appl. Phys. **64**, 2854 (1988).
[39]L. J. Guido, N. Holonyak, Jr., K. C. Hsieh, R. W. Kaliski, W. E. Plano, R. D. Burnham, R. L. Thornton, J. E. Epler, and T. L. Paoli, J. Appl. Phys. **61**, 1372 (1987).
[40]A. Furuya, O. Wada, A. Takamori, and H. Hashimoto, Jpn. J. Appl. Phys. **26**, L926 (1987).
[41]J. A. Van Vechten, in *Handbook on Semiconductors,* edited by S. P. Keller (North-Holland, Amsterdam, 1980), Vol. 3, pp. 76–80.
[42]J. A. Van Vechten, J. Appl. Phys. **53**, 7082 (1982).
[43]V. M. Vorob'ev, V. A. Murav'ev, and V. A. Panteleev, Sov. Phys. Solid State **23**, 653 (1981).
[44]F. A. Kröger, *The Chemistry of Imperfect Crystals* (North-Holland, Amsterdam, 1974), Vol. 2, pp. 7–9.
[45]G. A. Baraff and M. Schlüter, Phys. Rev. Lett. **55**, 1327 (1985).
[46]See, for example, B. I. Boltaks, *Diffusion in Semiconductors* (Academic, New York, 1963), pp. 7–9.
[47]J. A. VanVechten, in *Handbook on Semiconductors,* edited by S. P. Keller (North-Holland, Amsterdam, 1980), Vol 3, pp. 8, 9.
[48]C. Kittel and H. Kroemer, *Thermal Physics* (Freeman, San Francisco, 1980), p. 163.
[49]C. D. Thurmond, J. Electrochem. Soc. **122**, 1133 (1975).
[50]D. G. Deppe, N. Holonyak, Jr., K. C. Hsieh, P. Gavrilovic, W. Stutius, and J. Williams, Appl. Phys. Lett. **51**, 581 (1987).
[51]M. Kawabe, N. Shimizu, F. Hasegawa, and Y. Nannichi, Appl. Phys. Lett. **46**, 849 (1985).
[52]J. A. Van Vechten and C. D. Thurmond, Phys. Rev. B **14**, 3539 (1976).
[53]P. Mei, H. W. Yoon, T. Venkatesan, S. A. Schwarz, and J. P. Harbison, Appl. Phys. Lett. **50**, 1823 (1987).
[54]T. Y. Tan and U. Gösele, Appl. Phys. Lett. **52**, 1240 (1988).
[55]J. W. Lee and W. D. Laidig, J. Electron. Mater. **13**, 147 (1984).
[56]D. R. Myers, R. M. Biefield, I. J. Fritz, S. T. Picraux, and T. E. Zipperian, Appl. Phys. Lett. **44**, 1052 (1984).

[57]L. J. Vieland, J. Phys. Chem. Solids **21**, 318 (1961).
[58]G. R. Antell, Solid-State Electron. **8**, 943 (1965).
[59]M. E. Greiner and J. F. Gibbons, Appl. Phys. Lett. **44**, 750 (1984).
[60]P. Gavrilovic, J. Gavrilovic, K. Meehan, R. W. Kaliski, L. J. Guido, N. Holonyak, Jr., K. Hess, and R. D. Burnham, Appl. Phys. Lett. **47**, 710 (1985).
[61]K. L. Kavanagh, J. W. Mayer, C. W. Magee, J. Sheets, J. Tong, and J. M. Woodall, Appl. Phys. Lett. **47**, 1208 (1985).
[62]E. Omura, X. S. Wu, G. A. Vawter, L. Coldren, and J. L. Merz, Electron. Lett. **22**, 496 (1986).
[63]E. Omura, X. S. Wu, G. A. Vawter, E. L. Hu, L. A. Coldren, and J. L. Merz, Appl. Phys. Lett. **50**, 265 (1987).
[64]T. Morita, J. Kobayashi, T. Takamori, A. Takamori, E. Miyauchi, and H. Hashimoto, Jpn. J. Appl. Phys. **26**, 1324 (1987).
[65]L. J. Guido, W. E. Plano, D. W. Nam, N. Holonyak, Jr., J. E. Baker, and R. D. Burnham, J. Electron. Mater. **17**, 53 (1988).
[66]D. G. Deppe, N. Holonyak, Jr., and J. E. Baker, Appl. Phys. Lett. **52**, 129 (1988).
[67]K. Ishida, W. Matsui, T. Fukunaga, T. Takamori, J. Kobayashi, K. Ishida, and H. Nakashima, *Proceedings of the 13th International Symposium on GaAs and Related Compounds, Nevada*, 1986, edited by W. T. Lindley (Institute of Physics, Bristol, 1987), pp. 361–366.
[68]K. V. Vaidyanathan, M. J. Helix, D. J. Wolford, B. G. Streetman, R. J. Blattner, and C. A. Evans, Jr., J. Electrochem. Soc. **124**, 1781 (1977).
[69]D. G. Deppe, L. J. Guido, N. Holonyak, Jr., K. C. Hsieh, R. D. Burnham, R. L. Thornton, and T. L. Paoli, Appl. Phys. Lett. **49**, 510 (1986).
[70]D. G. Deppe, W. E. Plano, J. E. Baker, N. Holonyak, Jr., M. J. Ludowise, C. P. Kuo, R. M. Fletcher, T. D. Osentowski, and M. G. Craford, Appl. Phys. Lett. (to be published).
[71]E. W. Williams and F. B. Bebb, in *Semiconductor and Semimetals*, edited by R. K. Willardson and A. C. Beer (Academic, New York, 1972), Vol. 8, Chap. 5, pp. 359–377.
[72]C. J. Hwang, J. Appl. Phys. **40**, 4591 (1969).
[73]S. Y. Chiang and G. L. Pearson, J. Lumin. **10**, 313 (1975).
[74]D. T. J. Hurle, J. Phys. Chem. Solids **40**, 627 (1979).
[75]D. T. J. Hurle, J. Phys. Chem. Solids **40**, 639 (1979).
[76]C. W. Farley, T. S. Kim, S. D. Lester, and B. G. Streetman, J. Electrochem. Soc. **134**, 2888 (1987).
[77]J. Maguire, R. Murray, and R. C. Newman, Appl. Phys. Lett. **50**, 516 (1987).
[78]D. Laister and G. M. Jenkins, Philos. Mag. **23**, 1077 (1971).
[79]P. W. Hutchinson and P. S. Dobson, Philos. Mag. **30**, 65 (1974).
[80]D. L. Kendall, in *Semiconductors and Semimetals*, edited by R. K. Willardson and A. C. Beer (Academic, New York, 1968), Vol. 4, Chap. 3, pp. 205–225.
[81]H. C. Casey, Jr., in *Atomic Diffusion in Semiconductors*, edited by D. Shaw (Plenum, New York, 1973), Chap. 6, pp. 369–404.
[82]J. W. Allen and F. A. Cunnel, Nature **182**, 1158 (1958).
[83]F. A. Cunnel and C. H. Gooch, J. Phys. Chem. Solids **15**, 127 (1960).
[84]J. W. Allen, J. Phys. Chem. Solids **15**, 134 (1960).
[85]B. Goldstein, Phys. Rev. **118**, 1024 (1960).
[86]R. L. Longini, Solid-State Electron. **5**, 127 (1962).
[87]K. K. Shih, J. W. Allen, and G. L. Pearson, J. Phys. Chem. Solids **29**, 367 (1968).
[88]K. K. Shih, J. W. Allen, and G. L. Pearson, J. Phys. Chem. Solids **29**, 379 (1968).
[89]H. R. Winteler, Helv. Phys. Acta **43**, 496 (1970); **44**, 451 (1971).
[90]U. Gösele and F. Morehead, J. Appl. Phys. **52**, 4617 (1981).
[91]W. D. Laidig, N. Holonyak, Jr., J. J. Coleman, and P. D. Dapkus, J. Electron. Mater. **11**, 1 (1982).
[92]S. W. Kirchoefer, N. Holonyak, Jr., J. J. Coleman, and P. D. Dapkus, J. Appl. Phys. **53**, 766 (1982).
[93]M. D. Camras, N. Holonyak, Jr., K. Hess, M. J. Ludowise, W. T. Dietze, and C. R. Lewis, Appl. Phys. Lett. **42**, 185 (1983).
[94]W. D. Laidig, J. W. Lee, P. K. Chiang, L. W. Simpson, and S. M. Bedair, J. Appl. Phys. **54**, 6382 (1983).
[95]K. Meehan, J. M. Brown, M. D. Camras, N. Holonyak, Jr., R. D. Burnham, T. L. Paoli, and W. Streifer, Appl. Phys. Lett. **44**, 428 (1984).
[96]Y. Kawamura, H. Asahi, A. Kohzen, and K. Wakita, Electron. Lett. **21**, 219 (1985).
[97]K. Ishida, T. Ohta, S. Semura, and H. Nakashima, Jpn. J. Appl. Phys. **24**, L620 (1985).
[98]L. J. Guido, N. Holonyak, Jr., K. C. Hsieh, R. W. Kaliski, J. E. Baker, D. G. Deppe, R. D. Burnham, R. L. Thornton, and T. L. Paoli, J. Electron. Mater. **16**, 87 (1987).
[99]M. Razeghi, O. Archer, and F. Launay, Semicond. Sci. Technol. **2**, 793 (1987).
[100]K. Nakashima, Y. Kawaguchi, Y. Kawamura, Y. Imamura, and H. Asahi, Appl. Phys. Lett. **52**, 1383 (1988).
[101]D. G. Deppe, D. W. Nam, N. Holonyak, Jr., K. C. Hsieh, J. E. Baker, C. P. Kuo, R. M. Fletcher, T. D. Osentowski, and M. G. Craford, Appl. Phys. Lett. **52**, 1413 (1988).
[102]P. A. Houston, F. R. Shepherd, A. J. SpringThorpe, P. Mandeville, and A. Margittai, Appl. Phys. Lett. **52**, 1219 (1988).
[103]Y. Hirayama, Y. Horikoshi, and H. Okamoto, Jpn. J. Appl. Phys. **23**, 1568 (1984).
[104]T. Fukunaga, K. Ishida, T. Kuroda, K. Matsui, T. Narusawa, T. Morita, E. Miyauchi, H. Hashimoto, and H. Nakashima, *Proceedings of 12th International Symposium on GaAs and Related Compounds, Karuizawa, Japan*, 1985, edited by M. Fujimoto (Institute of Physics, Bristol, 1986), pp. 439–444.
[105]J. Kobayashi, M. Nakajima, Y. Bamba, T. Fukunaga, K. Matsui, K. Ishida, H. Nakashima, and K. Ishida, Jpn. J. Appl. Phys. **25**, L385 (1986).
[106]T. Venkatesan, S. A. Schwarz, D. M. Hwang, R. Bhat, M. Koza, H. W. Yoon, P. Mei, Y. Arakawa, and A. Yariv, Appl. Phys. Lett. **49**, 701 (1986).
[107]E. A. Dobisz, B. Tell, H. G. Craighead, and M. C. Tamargo, J. Appl. Phys. **60**, 4150 (1986).
[108]K. Matsui, J. Kobayashi, T. Fukunaga, K. Ishida, and H. Nakashima, Jpn. J. Appl. Phys. **25**, L651 (1986).
[109]J. Kobayashi, M. Nakajima, T. Fukunaga, T. Takamori, K. Ishida, H. Nakashima, and K. Ishida, Jpn. J. Appl. Phys. **25**, L736 (1986).
[110]L. J. Guido, K. C. Hsieh, N. Holonyak, Jr., R. W. Kalliski, V. Eu, M. Feng, and R. D. Burnham, J. Appl. Phys. **61**, 1329 (1987).
[111]S. A. Schwarz, T. Venkatesan, D. M. Hwang, H. W. Yoon, R. Bhat, and Y. Arakawa, Appl. Phys. Lett. **50**, 281 (1987).
[112]J. Kobayashi, T. Fukunaga, K. Ishida, H. Nakashima, J. D. Flood, G. Bahir, and J. L. Merz, Appl. Phys. Lett. **50**, 519 (1987).
[113]K. Ishida, E. Miyauchi, T. Morita, T. Takamori, T. Fukunaga, H. Hashimoto, and H. Nakashima, Jpn. J. Appl. Phys. **26**, L285 (1987).
[114]F. Brillouet, K. Ishida, T. Forita, E. Miyauchi, T. Takamori, and H. Nakashima, Jpn. J. Appl. Phys. **26**, 1320 (1987).
[115]D. R. Myers, G. W. Arnold, L. R. Dawson, R. M. Biefeld, C. R. Hills, and B. L. Doyle, Appl. Phys. Lett. **51**, 517 (1987).
[116]K. Ishida, K. Matsui, T. Fukunaga, J. Kobayashi, T. Morita, E. Miyauchi, and H. Nakashima, Appl. Phys. Lett. **51**, 109 (1987).
[117]K. Matsui, J. Kobayashi, T. Fukunaga, K. Ishida, and H. Nakashima, Jpn. J. Appl. Phys. **26**, L1122 (1987).
[118]D. Kirillov, P. Ho, and G. A. Davis, Appl. Phys. Lett. **48**, 53 (1986).
[119]J. Cibert, P. M. Petroff, D. J. Weider, S. J. Pearton, A. C. Gossard, and J. H. English, Appl. Phys. Lett. **49**, 223 (1986).
[120]J. Cibert, P. M. Petroff, G. J. Dolan, S. J. Pearton, A. C. Gossard, and J. H. English, Appl. Phys. Lett. **49**, 1275 (1986).
[121]G. Suzuki, Y. Hirayama, and H. Okamoto, Jpn. J. Appl. Phys. **25**, L912 (1986).
[122]D. J. Werder and S. J. Pearton, J. Appl. Phys. **62**, 318 (1987).
[123]K. Kash, B. Tell, P. Grabbe, E. A. Dobisz, H. G. Craighead, and M. C. Tamargo, J. Appl. Phys. **63**, 190 (1988).
[124]P. Mei, T. Venkatesan, S. A. Schwarz, N. G. Stoffel, J. P. Harbison, D. L. Hart, and L. A. Florez, Appl. Phys. Lett. **52**, 1487 (1988).
[125]D. R. Myers, G. W. Arnold, T. E. Zipperian, L. R. Dawson, R. M. Biefeld, I. J. Fritz, and C. E. Barnes, J. Appl. Phys. **60**, 1131 (1986).
[126]K. Meehan, N. Holonyak, Jr., R. D. Burnham, T. L. Paoli, and W. Streifer, J. Appl. Phys. **54**, 7190 (1983).
[127]K. Meehan, J. M. Brown, P. Gavrilovic, N. Holonyak, Jr., R. D. Burnham, T. L. Paoli, and W. Streifer, J. Appl. Phys. **55**, 2672 (1984).
[128]K. Meehan, J. M. Brown, N. Holonyak, Jr., R. D. Burnham, T. L. Paoli, and W. Streifer, Appl. Phys. Lett. **44**, 700 (1984).
[129]T. Fukuzawa, S. Semura, H. Saito, T. Ohta, Y. Uchida, and H. Nakashima, Appl. Phys. Lett. **45**, 1 (1984).
[130]K. Meehan, P. Gavrilovic, N. Holonyak, Jr., R. D. Burnham, and R. L. Thornton, Appl. Phys. Lett. **46**, 75 (1985).
[131]Y. Suzuki, Y. Horikoshi, M. Kobayashi, and H. Okamoto, Electron. Lett. **20**, 383 (1984).
[132]W. D. Laidig, J. W. Lee, and P. J. Caldwell, Appl. Phys. Lett. **45**, 485 (1984).
[133]H. Nakashima, S. Semura, T. Ohta, Y. Uchida, H. Saito, T. Fukuzawa, T. Kuroda, and K. L. I. Kobayashi, IEEE J. Quantum Electron. **QE-21**, 629 (1985).

[134]K. Meehan, P. Gavrilovic, J. E. Epler, K. C. Hsieh, N. Holonyak, Jr., R. D. Burnham, R. L. Thornton, and W. Streifer, J. Appl. Phys. **57**, 5345 (1985).
[135]P. Gavrilovic, K. Meehan, J. E. Epler, N. Holonyak, Jr., R. D. Burnham, R. L. Thornton, and W. Streifer, Appl. Phys. Lett. **46**, 857 (1985).
[136]S. Semura, T. Ohta, T. Kuroda, and H. Nakashima, Jpn. J. Appl. Phys. **24**, L463 (1985).
[137]S. Semura, T. Ohta, T. Kuroda, and H. Nakashima, Jpn. J. Appl. Phys. **24**, L548 (1985).
[138]H. Nakashima, S. Semura, T. Ohta, and T. Kuroda, Jpn. J. Appl. Phys. **24**, L647 (1985).
[139]P. Gavrilovic, K. Meehan, L. J. Guido, N. Holonyak, Jr., V. Eu, M. Feng, and R. D. Burnham, Appl. Phys. Lett. **47**, 903 (1985).
[140]D. G. Deppe, K. C. Hsieh, N. Holonyak, Jr., R. D. Burnham, and R. L. Thornton, J. Appl. Phys. **58**, 4515 (1985).
[141]R. L. Thornton, R. D. Burnham, T. L. Paoli, N. Holonyak, Jr., and D. G. Deppe, Appl. Phys. Lett. **47**, 1239 (1986).
[142]R. L. Thornton, R. D. Burnham, T. L. Paoli, N. Holonyak, Jr., and D. G. Deppe, Appl. Phys. Lett. **48**, 7 (1986).
[143]R. L. Thornton, R. D. Burnham,. T. L. Paoli, N. Holonyak, Jr., and D. G. Deppe, Appl. Phys. Lett. **49**, 133 (1986).
[144]D. G. Deppe, L. J. Guido, N. Holonyak, Jr., K. C. Hsieh, R. D. Burnham, R. L. Thornton, and T. L. Paoli, Appl. Phys. Lett. **49**, 510 (1986).
[145]Y. J. Yang, Y. C. To, G. S. Lee, K. Y. Hsieh, and R. M. Kolbas, Appl. Phys. Lett. **49**, 835 (1986).
[146]D. G. Deppe, G. S. Jackson, N. Holonyak, Jr., D. C. Hall, R. D. Burnham, R. L. Thornton, J. E. Epler, and T. L. Paoli, Appl. Phys. Lett. **49**, 883 (1986).
[147]K. Ishida, K. Matsui, T. Fukunaga, T. Takamori, and H. Nakashima, Jpn. J. Appl. Phys. **25**, L690 (1986).
[148]K. Ishida, T. Takamori, K. Matsui, T. Fukunaga, T. Morita, E. Miyauchi, H. Hashimoto, and H. Nakashima, Jpn. J. Appl. Phys. **25**, L783 (1986).
[149]R. L. Thornton, R. D. Burnham, T. L. Paoli, N. Holonyak, Jr., and D. G. Deppe, J. Cryst. Growth **77**, 621 (1986).
[150]R. L.Thornton, D. F. Welch, R. D. Burnham, T. L. Paoli, and P. S. Cross, Appl. Phys. Lett. **49**, 1572 (1986).
[151]L. J. Guido, G. S. Jackson, W. E. Plano, K. C. Hsieh, N. Holonyak, Jr., R. D. Burnham, J. E. Epler, R. L. Thornton, and T. L. Paoli, Appl. Phys. Lett. **50**, 609 (1987).
[152]D. G. Deppe, G. S. Jackson, N. Holonyak, Jr., R. D. Burnham, and R. L. Thornton, Appl. Phys. Lett. **50**, 632 (1987).
[153]D. G. Deppe, G. S. Jackson, N. Holonyak, Jr., D. C. Hall, R. D. Burnham, R. L. Thornton, J. E. Epler, and T. L. Paoli, Appl. Phys. Lett. **50**, 392 (1987).
[154]L. J. Guido, W. E. Plano, G. S. Jackson, N. Holonyak, Jr., R. D. Burnham, and J. E. Epler, Appl. Phys. Lett. **50**, 757 (1987).
[155]A. Furuya, M. Makuichi, O. Wada, T. Fujii, and H. Nobuhara, Jpn. J. Appl. Phys. **26**, L134 (1987).
[156]J. E. Epler, R. D. Burnham, R. L. Thornton, and T. L. Paoli, Appl. Phys. Lett. **50**, 1637 (1987).
[157]I. Ishida, E. Miyauchi, T. Morita, T. Takamori, T. Fukunaga, H. Hashimoto, and H. Nakashima, Jpn. J. Appl. Phys. **26**, L285 (1987).
[158]H. Nakashima and K. Ishida, Optoelectron. **2**, 235 (1987).
[159]J. E. Epler, R. D. Burnham, R. L. Thornton, and T. L. Paoli, Appl. Phys. Lett. **51**, 731 (1987).
[160]D. F. Welch, D. R. Scifres, P. S. Cross, and W. Streifer, Appl. Phys. Lett. **51**, 1401 (1987).
[161]D. G. Deppe, W. E. Plano, J. M. Dallesasse, D. C. Hall, L. J. Guido, and N. Holonyak, Jr., Appl. Phys. Lett. **52**, 825 (1988).
[162]F. Brillouet, E. V. K. Rao, and J. Beerens, Electron. Lett. **24**, 97 (1988).
[163]J. D. Ralston, L. H. Camnitz, G. W. Wicks, and L. F. Eastman, *Proceedings of the 13th International Symposium on GaAs and Related Compounds, Las Vegas,* 1986, edited by W. T. Lindley (Institute of Physics, Bristol, 1987), pp. 367–372.
[164]F. Julien, P. D. Swanson, M. A. Emmanuel, D. G. Deppe, T. A. DeTemple, J. J. Coleman, and N. Holonyak, Jr., Appl. Phys. Lett. **50**, 866 (1987).
[165]P. D. Swanson, F. Julien, M. A. Emmanuel, L. Sloan, T. Tang, T. A. DeTemple, and J. J. Coleman, Opt. Lett. **13**, 245 (1988).
[166]R. L. Thornton, J. E. Epler, and T. L. Paoli, Appl. Phys. Lett. **51**, 1983 (1987).
[167]B. C. Johnson, J. C. Campbell, R. D. Dupuis, and B. Tell, Electron. Lett. **24**, 182 (1988).